Dense Water Overflows and Cascades

by H. C. Mansley

Supervised by Prof. D. Marshall

September 1st, 2004

Declaration

I confirm that this is all my own work and that information obtained from other sources is appropriately acknowledged.

Abstract

This study reviews our current knowledge of the main physical processes affecting the dynamics and properties of dense water overflows and cascades in the ocean. Dense water formed by cooling, evaporation or sea-ice formation in the surface layer of the ocean descends into a deep ocean basin over sloping topography as an overflow or cascade. Large-scale overflows provide substantial contributions to globally important water masses that ventilate the abyssal ocean and force the global meridional overturning circulation. Our understanding of dense water overflows is far from comprehensive due a lack of observations and the complexity of their dynamics. Problems with resolution, mixing and bottom drag, and subsequent model dependence on simple parameterisations, lead to highly unrealistic representation of overflows in current ocean circulation and climate models.

Dense bottom flows descend under a balance of gravity, the Earth's rotation, bottom friction and turbulent entrainment. Overflows and cascades are predominantly in geostrophic balance and flow primarily alongslope with a small downslope component and viscous drainage in the bottom boundary layer. The weaker the rate of source water production, the greater the contribution of bottom friction to the source balance. Several different mechanisms enhance overflow dynamics, including the thermobaric effect, topographic features and suspended sediments. The downslope velocity of the dense flow is increased. Final depth reached may not increase due to the associated increase in entrainment and detrainment. The final product water that spreads into the ocean interior is insensitive to variations of the source water density due to a strong damping by corresponding changes in the rate of entrainment. Instead it largely depends on the thermohaline properties of the ambient water and the rate of its entrainment.

A simple plume model is used to illustrate the effects of bottom topography and friction in determining the path, the rate of descent, and the evolution of the thickness and width of the outflow. Entrainment and mixing is ignored. Once initialised, the model outflow is determined by the model dynamics and the bottom topography. Steeper regions do not allow the model flow to descend more quickly when an average gradient is maintained. The angle of descent is controlled by bottom drag and variable topography across the outflow affects the shape of the flow. Although this model is highly simplified, aspects of its behaviour are likely to be similar to that of overflows in current dissipative climate models.

Contents

Chapter 1

Introduction and Motivation

Very dense waters may be formed in the surface layer of the ocean through cooling, evaporation or sea ice formation over the continental shelf* or in a semi-enclosed or marginal sea [Condie, 1995]. The resulting horizontal density gradient drives an exchange flow between these dense waters and the open ocean [Ivanov et al., 2004]. The dense water enters a deep ocean basin, typically at a shallow depth, by overflowing the shelf edge or a topographic feature such as a strait and sill [Killworth, 2001] and must then descend the steep continental slope before reaching the open ocean.

It forms a density-driven bottom gravity current called an *overflow* or *cascade* [Killworth, 1983] and flows under a balance of gravity, the Earth's rotation and frictional forces [Whitehead, 1989]. An example of this process is shown schematically in Figure 1.1. As the overflow descends it entrains a substantial volume of the overlying oceanic water, which mixes with the dense water mass, modifying the temperature and salinity properties [Ivanov et al., 2004] and increasing its volume [Price and Baringer, 1994]. The intensity of this mixing and its effect varies greatly between outflows and the resulting *product* waters that finally disperse into the ocean interior may have quite different properties from the *source* waters that first entered the deep ocean basin.

*The continental shelf is an area of relatively shallow seawater on the edge of each continent, typically ending at a steep slope called the shelf break. The sea bottom below the break is the continental slope that has a much steeper gradient than the shelf and merges into the ocean floor.

The dense overflow descends to a depth where its density is equal to that of the ambient ocean water. This depth depends on its initial water mass properties and the entrainment and properties of surrounding water during its descent. The descended water leaves the slope and spreads isopycnally into the ocean interior either reaching the ocean bottom and becoming the bottom water mass, or forming intermediate depth layers [Ivanov et al., 2004].

Figure 1.1. Schematic of deep water formation in the Mediterranean Sea reproduced from Price [1992]

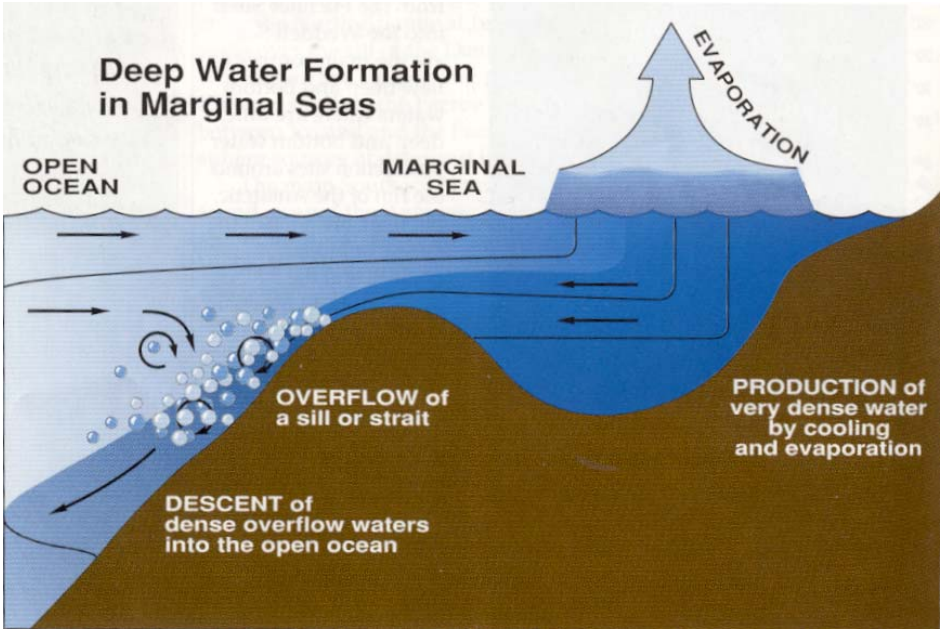

Cascading therefore provides a mechanism by which dense waters can efficiently descend into deep ocean basins. This process provides a crucial contribution to the ventilation and renewal of globally important abyssal water masses [Shapiro et al., 2003] that drive the deep global meridional overturning circulation [Condie, 1995].

Dense water overflows and the process of cascading are therefore of great current interest to a range of climatological applications and material transfer studies that are related to abyssal water formation and renewal [e.g. Rudels et al., 1999]. Accurate representation of overflows and their entrainment is vital for correctly representing deep water masses in general ocean circulation models and coupled climate models [Legg et al., 2004]. However, current model representation of dense water overflows is poor. Their complex dynamics coupled with difficulties in obtaining complete and useful observations mean that the impact of dense water overflows and their importance to water mass properties in the abyssal ocean are

still not fully understood. Research to understand and assess their contribution to deep water formation continues to be a major effort in oceanography.

The purpose of this study is to review our current knowledge of the main physical processes affecting the dynamics and properties of dense flows descending sloping topography. We begin in Chapter 2 with a brief discussion of the main processes contributing to dense water formation, the essential physical features of regions where this occurs, the contribution of observed overflows and cascades to abyssal water mass formation, and the main issues surrounding the inadequate representation of overflow dynamics in ocean models. In Chapter 3 we describe the balance of forces controlling the downslope propagation of the dense flow, and discuss the main processes affecting the density and volume properties of the overflow, the dependence of the product water on the properties of the source water, the ambient water, and the roles of entrainment and detrainment. A simple plume model is used in Chapter 4 to isolate and analyse the roles of bottom topography and friction in determining the path, the rate of descent, and the evolution of the thickness and width of the outflow. We conclude with a discussion of future work needed to improve our understanding of both dense overflow processes and climate.

Chapter 2

Deep Ocean Exchange

2.1. Introduction

The World Ocean is very stably stratified, with warmer waters at the surface and colder waters below. The abyssal ocean below the thermocline is insulated from direct atmospheric forcing and here density gradients drive much of the circulation. In particular, the thermohaline circulation is a global meridional overturning circulation thought to be the main system able to renew or change the properties of the abyssal ocean waters [Price, 1992]. In turn the thermohaline circulation is driven by inputs of dense water [Dickson and Brown, 1994] and one of the main processes feeding the thermohaline circulation is deep convection [Killworth, 1983].

There are two types of deep convection occurring in the World Ocean: open ocean convection and slope convection, the latter is also referred to as cascading. Open ocean convection involves predominantly vertical flows and takes place far from land, occurring in semi-enclosed and marginal seas such as the Mediterranean Sea, the Labrador Sea [Killworth, 1983] and the Greenland Sea [Rudels and Quadfasel, 1991]. Cascading occurs near ocean boundaries and involves dense water formed in shallow surface regions or in semi-enclosed or marginal seas, overflowing the continental shelf edge or a topographic feature such as a strait or sill, and descending the continental slope. These outflows are able to transport dense water into the abyssal ocean with much less turbulence and local mixing than would occur if the water flowed directly into the ocean interior [Killworth, 2001]. A schematic of this process is shown in Figure 1.1.

2.2. Dense water formation

Density variations in the global oceans arise directly from variations in temperature and salinity [Price, 1992]. Cold and saline waters are denser than warm and fresh waters. Intense and sustained air-sea exchange of heat and fresh water is needed to achieve sufficiently dense surface waters needed to drive deep convection and form abyssal waters [Shapiro and Hill, 1997]. This can occur most effectively in particular regions over the shallow areas of the continental shelf and in semi-enclosed or marginal seas rather than in the adjacent deep waters of the open ocean due to a number of features [Shapiro et al., 2003].

Ocean-shelf exchange tends to be inhibited by sills and straits or the steep bathymetry at the shelf edge. Currents varying on time-scales longer than a day tend to flow horizontally along depth contours in geostrophic equilibrium as downslope buoyancy forces are balanced by the upslope Coriolis force and shelf waters and marginal seas are therefore partially separated from the horizontal circulation and stirring of the open ocean [Price, 1992].

Typically, strong winter winds blow cold, dry air off the nearby land resulting in intense cooling or evaporation [Lazier et al., 2001], such as that resulting from winds blowing off the ice-sheet in the Labrador Sea [Clarke and Gascard, 1983; Seung, 1987]. Enclosed seas are also more likely to have a more severe continental and therefore dry winter climate [Price, 1992]. The marginal seas waters are also subject to weak cyclonic circulations confining the water and sustaining heat loss from the same body of water [Lazier et al., 2001].

The reduced heat capacity of shallow regions results in a much larger temperature change for the same heat flux than in the surrounding deeper regions [Condie, 1995]. Similarly, evaporation or sea ice formation and the accompanying brine rejection in shallow areas results in much more saline, and therefore denser water than in the open ocean [Shapiro et al., 2003], such as the very salty waters resulting from evaporation in the Mediterranean Sea. Sea ice formation in high latitudes is also enhanced in winter by the larger temperature change experienced over the continental shelf and is particularly efficient in regions of divergent ice movement such as coastal polynyas that are formed and sustained by the offshore winds [Schauer and Fahrbach, 1999].

The favourable conditions for dense water formation coupled with inhibited ocean-shelf exchange allow dense *source* waters to accumulate within depressions on the shelf or in marginal seas. Convective mixing

due to atmospheric forcing in shallow areas, where the water depth is less than the depth of penetrating convection, can create a nearly homogenous mass of cold or salty dense water [Shapiro et al., 2003].

2.3. Exchange flows

Dense water formation creates a horizontal density contrast between the dense shelf or marginal sea waters and the lighter ambient deep water, which can be extremely strong and extend to the bottom layer [Shapiro et al., 2003]. The local density increase induces a horizontal pressure gradient that drives the dense water towards the shelf edge or open ocean [Schauer, 1999].

Upon reaching the shelf edge or passing through a sill or strait from a marginal sea, the dense source water spills into a deep basin, often entering at a shallow depth [Lane-Serff, 2001], cascading down the continental slope or into another ocean basin as a turbulent gravity current [Killworth, 2001]. Cascading occurs at a range of scales [Killworth, 1983] and large-scale continuous flows are referred to as 'overflows', while smaller scale, intermittent flows are referred to as 'cascades' [Lane-Serff, 2001]. A section of a dense cascading flow extending to the bottom of the slope is shown in Figure 2.1 [Muench and Gordon, 1995].

Figure 2.1. Potential temperature (left) and salinity (right) for the oceanographic section across the Antarctic continental slope at a location in the southern Weddell Sea (68ºS, 53ºW) showing dense bottom downslope flow [reproduced from Muench and Gordon, 1995].

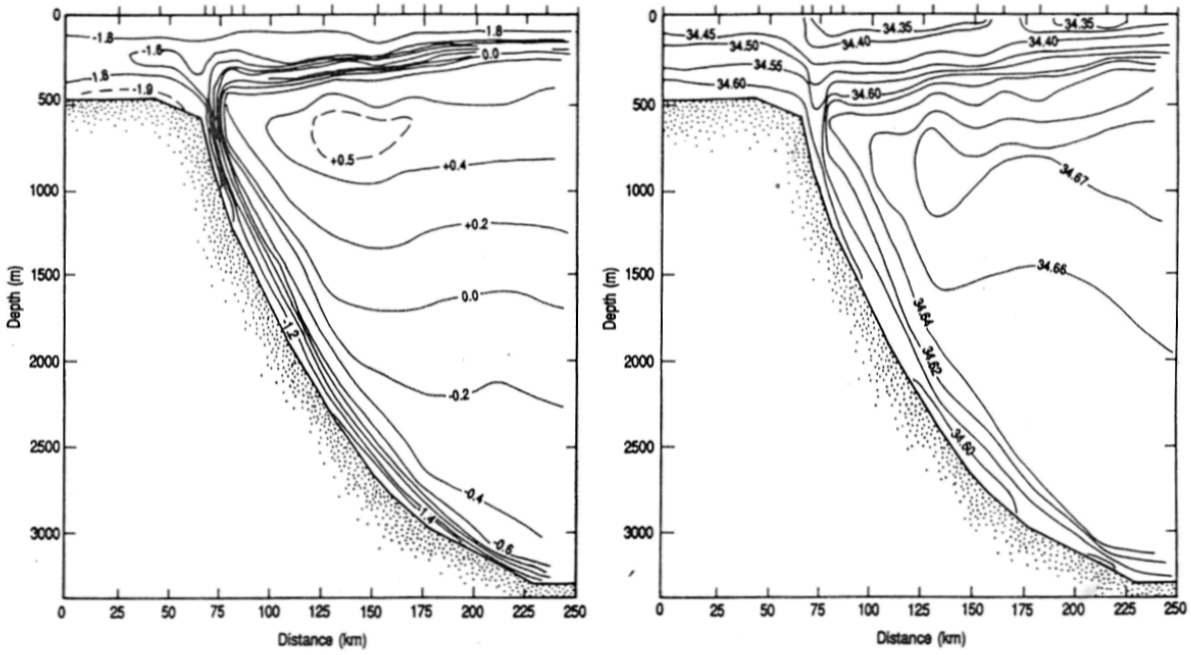

The resulting flows produce an irreversible exchange between ocean and shelf or sea waters [Shapiro et al., 2003]. In the Faroe Bank Channel outflow and the Mediterranean outflow, the rate of exchange appears to depend only upon this density contrast between the marginal sea and the open ocean, and the width and depth of the Gibraltar strait [Price, 1994] with lighter Atlantic waters entering from the open ocean at the surface and denser Mediterranean water flowing out beneath [Lane-Serff, 2001]. However, the exchange can be more complex and may also include a contribution from the ocean basin circulation. This is thought to be the case for the outflows through the Denmark Strait and from the Weddell Sea, which do not appear to have simple two-layer exchange [Price, 1994].

Cascading thus provides a mechanism by which dense waters formed at the surface can flow from the continental shelf or marginal sea into an ocean basin, or from one ocean basin down into another one [Lane-Serff, 2001]. Although vertical ocean exchange is also generated by, for example, flow over topography, tides and internal waves, significant vertical mixing over most of the ocean is confined to these topographically complex boundary areas [Wunsch, 2004]. This is supported by results such as those of Toole, Polzin and Schmitt [1994] who estimated diapycnal mixing in the deep ocean interior to be 1 to 2 x 10^{-5} m^2s^{-1} in contrast with values greater than 10^{-4} m^2s^{-1} found near steep slopes. As such, the mixing occurring downstream of overflows dominates the mixing of abyssal waters [Lane-Serff, 2001] and turbulent dense water overflows descending the continental slope are therefore influential in water-mass formation. They provide a substantial contribution to intermediate and deep waters and are responsible for ventilating several globally important abyssal water masses [Schauer, 1995; Ivanov et al., 2004], and hence exert a controlling influence on the stratification.

The dynamics of cascading are essential to maintaining a stably stratified world ocean [Killworth, 1983] and the global meridional overturning circulation [Lazier et al., 2001]. Overflows and the cascading process are as such of great current interest. They take an important role in transfer of suspended material and dissolved gasses, removing nutrients, organic particles and pollutants from productive areas on continental shelves and transporting them to the deep ocean [Condie, 1995; Huthnance, 1995]. It is also believed that cascading may assist turbidity currents in transporting sediments to the deep sea, although there are no accurate estimates [Shapiro et al., 2003]. This is of great importance to various climatological applications, studies of nutrient fluxes [Shapiro et al., 2003], biogeochemical cycles such as carbon cycling, and ocean-shelf material transfer [Ivanov et al., 2004], which are related to intermediate and deep water formation. In addition, it is known that deep convection, and hence cascading in the ocean modifies the global climate on long time scales and provides a buffer to long term climatic variability since it can take decades or more for the subducted water to resurface [Shapiro et al., 2003].

2.4. Observed overflows and cascades

Although dense water formation and outflows down steep topography are a widespread occurrence in the global oceans [Shapiro and Hill, 1997; Lane-Serff, 2001], not all may contribute to the ventilation of the abyssal ocean layers. Dense water produced over the continental shelf may be far from the open ocean and must propagate a large distance across the shelf before reaching the steep continental slope. Its transport over a gently sloping or flat bottom, such as that of the shelf, is generally quite slow and there may be a relatively long interval between dense water formation and the initiation of cascading [Shapiro and Hill, 1997]. On its path, the dense water will entrain considerable amounts of relatively light ambient shelf water before reaching the slope [Schauer and Fahrbach, 1999] and could partially lose its density excess. This may lead to weaker cascading or the dense flow not reaching the slope [Shapiro et al., 2003]. For example, dense water may be produced very effectively at sites such as near the Central Bank in the Barents Sea [Quadfasel et al., 1992], but may not ventilate the deep ocean since it loses its density excess during its several hundred kilometre journey toward the shelf edge. A comprehensive study by Ivanov et al. [2004] identified sixty-one confirmed cascades worldwide, including twenty-five cases in the Arctic Seas, seventeen off the Antarctic shelves, twelve at mid-latitudes and seven in sub-tropical and tropical regions. Examples of cascades include inflows over sills into the Black Sea [Latif et al., 1991] and the Baltic Sea [Lundberg, 1983]. Cascades of dense water formed in shelf seas include the Bass Strait and Spencer Gulf, Australia [Tomczac, 1985] and the Adriatic Sea [Zoccolotti and Salusti, 1987]. Mesoscale cascades and their associated mixing may be influential in water mass formation, but their contribution cannot be estimated from current observations of production and slope convection of shelf waters and remains unquantified [Ivanov et al., 2004].

Most of the cold, polar and subpolar waters that fill the abyssal ocean have originated from one of several important marginal sea outflows; the Denmark Strait and Faroe Bank Channel outflows from the Norwegian and Greenland Seas, and at least one outflow around Antarctica from the Filchner Ice Shelf into the Weddell Sea and subsequently into the Southern Ocean [Baringer, n.d.]. Dense water overflows from these regions are crucial to the formation of abyssal waters. Antarctic Bottom Water comprises or contributes to most of the deep waters of the world ocean and is the most widespread water mass in the world [Killworth, 1983]. Various sites on the continental shelf of Antarctica contribute to the formation of Antarctic Bottom Water [Baines and Condie 1998; Gordon et al., 1998), although much of the cold dense water is generally believed to be principally formed in the Weddell Sea, and in particular, over the Filchner Ice Shelf [e.g. Dickson and Brown, 1994]. However, Baines and Condie [1998] suggest that

dense bottom flows outside the Weddell Sea could be thin, due to a lack of topographic constraints, and thus difficult to detect. Their contribution may therefore be larger than previously thought and comparable to that from the Weddell Sea.

Figure 2.2. A schematic of the forcing the Atlantic thermohaline circulation by the principal overflows [reproduced from Price, 1992]

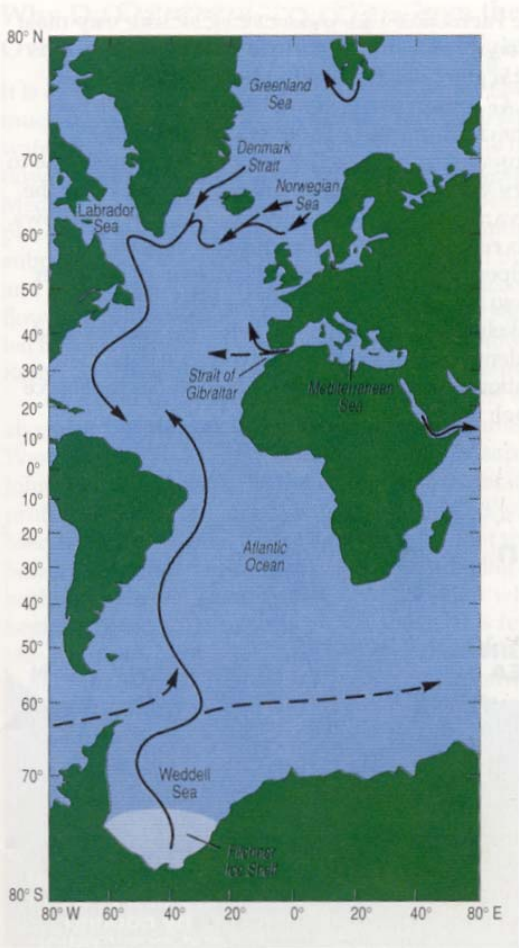

Overflows off the vast Arctic shelves provide essential contributions to the ventilation of deep and intermediate layers of the Norwegian and Greenland Seas, and the Artic Ocean. Backhaus et al. [1997] discuss their importance, which has also been inferred from analyses of water masses and tracers of the Arctic Ocean [e.g. Bauch et al., 1995]. The dense overflows through the Denmark Strait [e.g. Jungclaus and Backhaus 1994] and Faroe Bank Channel [Fogelqvist et al., 2003] are critical to the formation of North Atlantic Deep Water [Dickson and Brown, 1994] and Arctic Intermediate Water [Shapiro et al., 2003]. In addition, the overflows from the Labrador Sea and Mediterranean Sea are considered to be

major sources of intermediate water entering the North Atlantic [Price, 1994]. A schematic of the abyssal circulation in the Atlantic forced by the principal overflows is shown in Figure 2.2.

Model results [e.g. Döscher and Redler, 1997] indicate that deep water formation below the Greenland-Iceland-Scotland ridge does not significantly force the large-scale Atlantic Meridional Overturning Circulation. Antarctic Bottom Water and North Atlantic Deep Water predominantly force the global thermohaline circulation [Dickson and Brown, 1994] and results such as these suggest the essential role of overflows in ventilating and renewing these globally important abyssal water masses in the world oceans and eventually in shaping the global meridional overturning circulation [Shapiro et al., 2003].

2.5. Key issues for climate modelling

Despite its global importance, convective processes responsible for deep and intermediate water formation along the continental margin are not well understood. There are many difficulties associated with obtaining complete and useful observations of cascading. Poor winter weather conditions in the Arctic and Antarctic, where most cascading occurs, and at times complete ice coverage of overflows contribute to the difficulties in obtaining observations. It takes place in the bottom layers of the ocean and cannot be traced using satellites [Shapiro et al., 2003]. In areas with abrupt and dissected bathymetry, such as the east Greenland slope, it is difficult to reposition observational equipment at equivalent depths and locations in successive years, and thus construct a valid time series from which to estimate variability of the outflow [Dickson and Brown, 1994]. Dense cascades are also often intermittent in time and space and as such may be composed of individual mesoscale events that are rarely observed while in progress [Huthnance, 1995; Shapiro and Hill, 1997; Ivanov et al., 2004].

It is known from observations that dense water cascading down a slope encounters a number of different water masses [Killworth, 1983]. Observational [Girton and Sanford, 2003] and laboratory studies [Cenedese et al., 2004] of dense bottom gravity flows suggest the density contrasts involved, and their interaction with steep bathymetry and rotation produce complicated flow dynamics, particularly near the shelf edge, that may involve eddy formation, bottom mixing and turbulent entrainment [Ezer, 2004]. The Denmark Strait overflow, for example, exhibits intense entrainment with highly variable currents and transport rates within 100–200 km from the Greenland-Iceland ridge [Girton and Sanford, 2003].

The complex nature of cascading coupled with few available direct observations means that the impact of dense bottom gravity currents on the global overturning circulation and their importance to water properties of the deep ocean remains unquantified [Lazier et al., 2001]. However, the thermohaline

circulation is sensitive to the dynamical details of large-scale overflows [e.g. Döscher and Redler, 1997; Willebrand et al. 2001], and it is certain that they are integral to the formation of important water masses.

Realistic modelling of overflows is therefore necessary for accurate representation of deep sea ventilation and credible climate modelling [Legg et al., 2004]. However, the complex nature of overflow dynamics leads to many modelling challenges in order to accurately simulate such flows. Simplified process orientated models can reveal a particular mechanism of a cascade from comparing model results against the observed data [e.g. Hill et al., 1998], but current representation of the deep sea in ocean circulation and coupled climate models is highly unrealistic [Shapiro et al., 2003; Condie, 1995]. Despite recent laboratory and numerical investigations developing our physical understanding of the dynamics of dense water overflows [Lane-Serff, 2001], overflow simulations are usually based on extremely simple parameterisations because of problems with resolution, mixing and bottom drag [Condie, 1995]. Simulations are thus largely dependent on the subgrid-scale mixing parameterization [Griffies et al., 2000] and the model configuration [Ezer, 2004]. These problems are heightened for coarse resolution climate models [Ezer, 2004]. Research to further understand and assess the contribution of dense water overflows and cascades to deep water formation and the ventilation of the deep sea continues to be a major effort in oceanography.

2.6. Summary

Intense and sustained atmospheric forcing is required to form extremely dense surface waters. Conditions are most favourable for dense water production in shallow regions and in semi-enclosed or marginal seas. Under present climatic conditions, the densest waters are produced at high latitudes. The resulting horizontal pressure gradient induces an exchange flow with the open ocean. The dense fluid forms a turbulent bottom current, which descends into a deep ocean basin over sloping topography. Vertical mixing in the ocean occurs principally in these steep slope boundary regions and thus dense water overflows are influential in abyssal water mass formation. In particular, large-scale dense overflows in the Arctic and from a handful of important marginal seas provide substantial contributions to globally important water masses. Most essentially, to Antarctic Bottom Water and North Atlantic Deep Water, which predominantly ventilate the abyssal ocean and force the global thermohaline circulation. Overflows are of great relevance to a range of climate and material transfer applications that are related to abyssal water formation and renewal.

Our understanding of dense water overflows is far from comprehensive, largely because of the difficulties associated with obtaining observations and the complexity of their dynamics. Importantly, the contribution of mesoscale cascades to dense water mass formation is unknown. Problems with resolution, mixing and bottom drag, and subsequent model dependence on simple parameterisations, lead to highly unrealistic representation of overflows in current ocean circulation and climate models. To remedy this we must first develop a physical understanding of the fundamental dynamical processes occurring in overflows. In the next chapter, we shall review current knowledge of the main processes affecting dense overflow dynamics.

Chapter 3

Dynamics of overflows: theories, experiments and observations

3.1. Introduction

Dense water cascading down sloping bathymetry is an extremely complex phenomenon involving numerous mesoscale processes and effects. Overflows and cascades are density driven and therefore any process that alters their density affects their evolution, in particular, the volume and tracer properties, the path taken and the final depth reached. We thus expect the dense plume to distort in a complex way over time because of local effects [Shapiro and Hill, 1997].

In this chapter, a combination of theories, observations and results from laboratory experiments and numerical models is used to provide a review our current knowledge of the main physical processes affecting the dynamics and properties of dense water outflows. We first describe the balance of forces controlling the downslope propagation of the dense flow and examine a variety of downslope transport mechanisms. We consider physical characteristics of the dense flow, the bathymetry, and the ambient water that can affect the force balance and discuss their main effects. The final product water that disperses into the ocean interior is very different from the source water before its descent. This is of particular importance to the depth reached by the overflow and its associated transports. We identify the main processes affecting the density and volume properties of the overflow. We further discuss the dependence of the product water on the properties of the source water and the ambient water, and the roles of entrainment and detrainment.

3.2. Forces controlling the flow

On the continental shelf, frictional forces are relatively small and in steady state conditions dense water flow over a relatively large horizontal scale (~10 km) is in geostrophic balance and horizontal along density fronts [Gill, 1982]. This tends to produce a front at or near the shelf break separating dense shelf water from lighter off shelf waters. However, dense water not originally in geostrophic balance undergoes geostrophic adjustment close to the source, which can cause cross slope propagation of the plume [Shapiro et al., 2003]. In regions with sufficiently large and extensive dense water production on the continental shelf, geostrophic adjustment may extend off the shelf and cause the front to descend the continental slope [Baines and Condie, 1998].

As the dense water spills onto the continental slope through a topographic constriction, such as a sill or strait, or from the continental shelf, geostrophy should continue to dominate the cross-stream balance throughout the transition onto the slope and during its longer-term development. With the influence of the Earth's rotation preventing the dense fluid from flowing downslope, on a sloping bottom we would expect the dense water plume to move along slope following contours of constant depth [Nof, 1983].

A dense outflow not in geostrophic balance at the top of the continental slope would therefore initially accelerate directly downslope under the influence of gravity. For geostrophic adjustment already underway, there is also an along slope component. The effects of the Earth's rotation deflect the flow, causing it to curve to the left in the Southern hemisphere and right in the Northern hemisphere, and eventually flow along the slope at a constant depth. The distance over which the geostrophic adjustment from downslope to alongslope flow takes place scales with the Rossby radius of deformation [Lane-Serff, 2001].

3.3. Downslope transport processes

However, the overall dynamics and especially the dynamics of the bottom layer on the continental slope are strongly influenced by ageostrophic effects [Shapiro and Hill, 1997]. The complex balance of forces affecting the evolution of the outflow, namely gravity, the Earth's rotation, bottom friction and turbulent entrainment, are altered on the steep continental slope. The presence of steep bottom topography and friction enables an ageostrophic downslope component of flow [Shapiro and Hill, 1997]. Enlarged bottom friction, eddy formation and increased turbulent mixing affect the outflow, causing cascading down the continental slope. In reality, both dense overflows and cascades form particular types of gravity currents in a rotating system [Shapiro et al., 2003].

3.3.1. Friction

A dense bottom flow becomes more energetic on the steep continental slope due to gravitational acceleration [Ivanov et al., 2004]. Flow speeds can be 10-100 times faster than most other deep ocean flows [Lane-Serff, 2001] and friction is considerably increased in this region. In consequence, friction is no longer negligible as on the continental shelf.

Friction over sloping topography is essential since it breaks the constraint of potential vorticity conservation that would require all motion to be along depth contours and therefore alongslope [Shapiro and Hill, 1997]. It disrupts geostrophy and although most motion is still alongslope, part of the downslope reduced-gravity force is now unbalanced by rotation and allows it to drive downslope motion. This process, whereby friction brings about a density-driven downslope component of flow is cascading [Shapiro and Hill, 1997]. Measurements of bottom drag on the slope show that the core path of the dense overflow supports a rate of descent controlled by friction [Girton and Sandford, 2003].

3.3.2. Entrainment

The increased flow speeds and friction on the continental slope generates additional turbulence, increasing both entrainment of ambient waters into the overflow and detrainment of dense fluid. A number of models, such as that of Smith [1975] and Price et al. [1993], add a retardation due to entrainment to the bottom friction term which increases the cross contour angle from that of bottom friction alone. In these models, the contribution of entrainment is most influential during the initial descent of the dense flow near the source, where the outflow is experiencing strong entrainment due to geostrophic adjustment [Dickson and Brown, 1994]. This suggests the dominance of bottom friction as a control on the angle of descent after the outflow becomes steady.

3.3.3. Drainage in Ekman Layer

Forced Ekman drainage is the transport induced by the Ekman veering of an upper-layer along slope current impinging on the seabed (e.g. a barotropic eastern boundary current). It allows water to leak away perpendicular to the direction of the main current, to the left in the Northern hemisphere and the right in the Southern hemisphere. It can therefore bring about downslope motion in the thin bottom boundary layer (the Ekman layer) over sloping topography known as Ekman drainage [Shapiro and Hill, 1997; Condie, 1995].

Fluid in the bottom Ekman layer is preferentially drained from the upslope side of the dense plume, gradually shifting the main flow downslope in addition to its existing downslope progress [Baines and Condie, 1998]. On the continental shelf, where the bottom gradient is slight, the density-driven propagation of the dense water is slow. Laboratory experiments have highlighted the weakness of density-driven flow over areas with little or no slope, such as the continental shelf. Here drainage is likely to prevail over cascading as a downslope forcing mechanism.

3.3.4. Baroclinic instability

Simulated dense flows [Jiang and Garwood, 1996] and those of laboratory experiments [Smith, 1977; Condie, 1995; Lane-Serff and Baines, 1998] are extremely unstable and under certain conditions, in particular where the thickness of the dense layer is much greater than that of the Ekman layer, may result in the formation of strong eddies [e.g. Jiang and Garwood, 1995; Gawarkiewicz and Chapman, 1995].

Taylor columns of ambient water can be carried into deeper water by the bottom downslope flow undergoing geostrophic adjustment near the source and Ekman drainage, or alternatively as a result of instability in the along slope flow, such as baroclinic instability further downstream [Gill, 1982]. The water column is stretched and becomes thinner, generating cyclonic vorticity in the column in order to conserve angular momentum, as demonstrated schematically in Figure 3.1 [Lane-Serff, 2001]. This results in cyclonic circulation above the dense fluid, and relatively weaker cyclonic, or even anticyclonic circulation within it [Lane-Serff and Baines, 1998]. These circulations are not limited to the waters immediately around the overflow and can occupy the whole water column, forming eddies that may be visible at the sea surface hundreds of metres above the overflow [Lane-Serff, 2001].

This may disrupt the continuous dense overflow below and break it up into a number of domes that propagate along the slope with eddies above at the surface [Lane-Serff, 2001]. Vigorous unstable eddies are confined to the upper slope region in steep slope cases, while they cover the whole slope region in gentle slope cases, due to the balance between the opposing stabilizing and destabilizing effects of the bottom slope [Tanaka and Akitomo, 2001]. These eddies continue to lose fluid to drainage and have been observed in the Denmark Strait overflow [Bruce, 1995; Krauss, 1996]. Both models and experiments show that baroclinic waves and eddies are an important feature of dense bottom flows which are highly unstable, particularly in the initial accelerating stage as a consequence of geostrophic adjustment [e.g. Jiang and Garwood, 1995; Gawarkiewicz and Chapman, 1995]. Eddy fluxes dominate the downslope transport [Baines and Condie, 1998] and although eddy transports for steep slopes are much less than for gentle slopes they are still larger than that due to the Ekman drainage [Tanaka and Akitomo, 2001].

In addition, stratification of the ambient water increases the stretching parameters and increases eddy production. There are also indications that the eddy propagation speed along the slope is lessened by stratification, possibly due to internal wave generation [Lane-Serff, 2001].

Figure 3.1
Columns of fluid, figure 4 [reproduced from Lane-Serff, 2001]

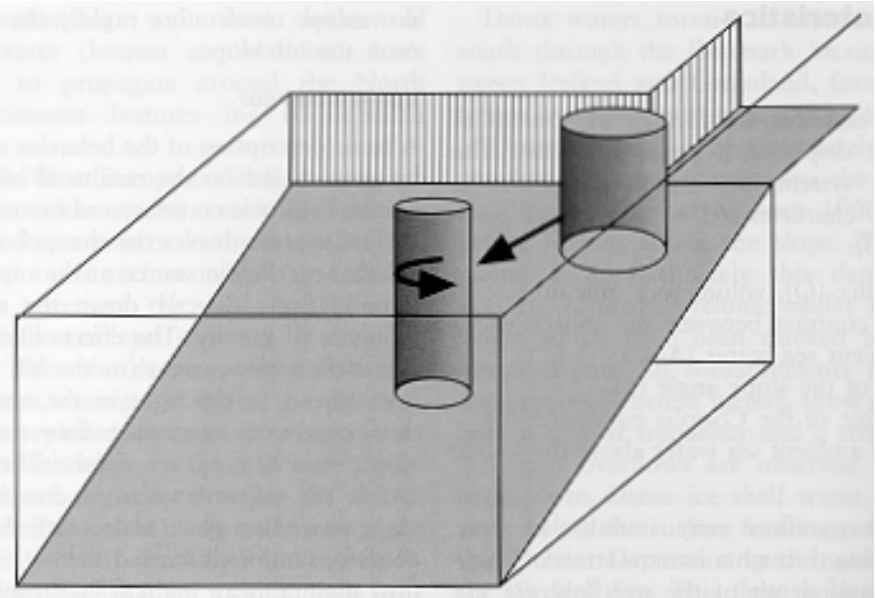

3.4. Downslope transport regimes

Model results such as those of Shapiro and Hill [1997] confirm that dense water cascading down the continental slope distorts in a complex way over time as a result of the local processes discussed. Baines and Condie [1998], and Shapiro and Zatsepin [1997] concluded, from analysing observations and model results, that there are several regimes of downslope propagation of a dense outflow descending sloping bathymetry. Outflows are categorized into a regime based on a rate of source water production. These are defined quantitatively by Baines and Condie [1998].

3.4.1. Regime one

For a sufficiently intense and continuous source of dense water, a combination of the continual supply of fluid at the top of the slope and geostrophic adjustment of the flow can force the fluid downward. The dense outflow descends as a thick broad sheet for an extensive source, or a plume for a more local source [Baines and Condie, 1998].

The relative importance of viscous effects is connected to the ratio of the boundary layer thickness to the thickness of the dense outflow. For an intense supply, the dense plume or sheet is thick (compared to the thickness of the Ekman layer) and therefore bottom friction effects are relatively unimportant to the motion of the plume [Baines and Condie, 1998; Shapiro and Hill, 1997].

For this reason, along slope flow is in approximate inviscid geostrophic balance over most of the depth of the layer, with externally imposed currents driving thick plumes in the direction of flow [Shapiro and Hill, 1997]. The dense fluid is still continuously drained at its base by the viscous bottom layer, which takes fluid from the base of the current at an angle down the slope [Lane-Serff, 2001]. However, water transports within the Ekman layer account for only a small portion of the total downslope transport [Baines and Condie, 1998; Shapiro and Hill, 1997] and the evolution of the near inviscid outflow is therefore mostly governed by geostrophy, and mixing [Condie, 1995].

In summary, an intense level of dense water production creates a thick broad plume or sheet on the continental slope in which eddies may form. The outflow is mostly governed by geostrophy and the long-term density driven evolution of the dense water on sloping topography is principally along slope. It is continuously drained in the Ekman layer and the outflow stretches from the source, in a sheet, plume or in a series of domes, mostly along depth contours and slightly down slope [e.g. Jungclaus and Backhaus, 1994] until it reaches the bottom, or its own density level. A schematic of this process is shown in Figure 3.2.

3.4.2. Regime two

With a moderate level of production where the dense water supply is not as great or as extensive, alongshore gradients in the flow, buoyancy forcing or bathymetry may cause the dense fluid to spill over the shelf edge. The moderate supply produces thinner plumes or filaments whose upslope boundary is not attached to the source [Baines and Condie, 1998].

For a moderate source and thus thin plumes, the geostrophy balance partially applies [Shapiro et al., 2003]. Thinner sheets or plumes are, however, relatively more strongly influenced by boundary layer processes. Friction is much more important and the evolution of the outflow and overall motion is more ageostrophic. The increased importance of viscous effects restricts the along slope velocities and viscous downslope transport in the Ekman layer comprises a larger component of the overall downslope motion [Shapiro and Hill, 1997]. The density-driven downslope motion is stronger and along slope flow is

correspondingly reduced. In a thinner layer, friction restricts the growth of baroclinic instabilities and thus eddy production [Condie, 1995; Lane-Serff and Baines, 1998]. Eddy transport provides a smaller component of the downslope motion than Ekman drainage. The descent of the plume or filament down sloping bathymetry is, however, predominantly geostrophic and most of the downslope transport is above the boundary layer.

Figure 3.2. A schematic diagram of the descent of dense water, formed over the continental shelf, down the continental slope as a sheet, with eddy formation and Ekman drainage, or as a plume in a submarine canyon. All these processes may not be occurring simultaneously and for a localised outflow, the dense water would descend as a plume [reproduced from Baines and Condie, 1998].

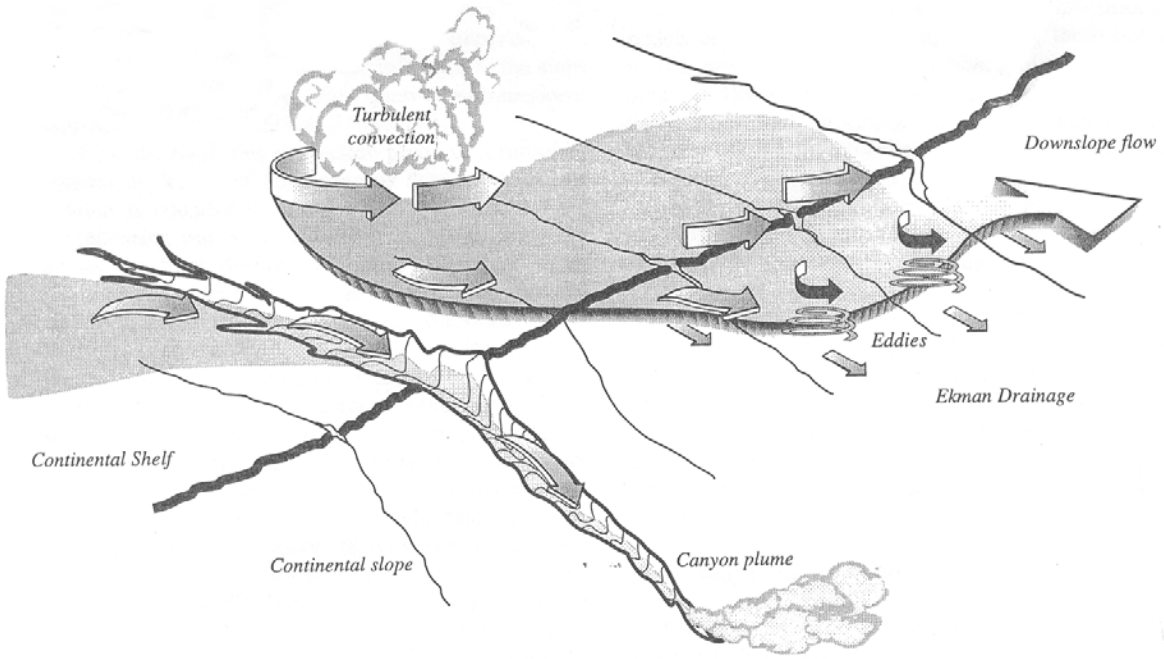

3.4.2. Regime three

A weak dense water supply, where the discharge per unit length of slope is less than or equal to the downslope Ekman transport, is weak enough to be balanced by Ekman drainage. Viscous effects become important with the only transport being viscous drainage within the Ekman boundary layer [Shapiro et al., 2003]. A thin layer extends down the slope until it reaches to its own density level or is eroded by turbulent mixing [Baines and Condie, 1998].

Transition between these regimes may occur as the dense flow varies with time or distance along slope due to detrainment or steepening topography [Baines and Condie, 1998]. This theory provides several

insights into the overflow process. Cascading is to a high degree related to geostrophic along-slope flow. In many overflows, the effect of the bottom friction is constrained to a bottom boundary layer and viscous down-slope motion is mostly confined to within this lower layer [Condie, 1995; Shapiro & Hill, 1997; Whitehead, 1993]. However, there are some strong turbulent overflows, such as the Mediterranean overflow in which properties are well mixed.

An intense source producing a thick broad plume fits well with the large-scale overflows from marginal seas, for example the Weddell Sea or through the Denmark Strait where the predominant balance is geostrophic and frictional effects are relatively small. Cascades, which tend to be episodic and are smaller in magnitude than overflows, are not dynamically analogous to large-scale dense water outflows. Although cascades are similarly affected by the Earth's rotation and also flow along rather than directly down slope, the important difference is a larger contribution from the bottom friction to the force balance [Shapiro et al., 2003].

3.5. The thermobaric effect

The thermal expansion coefficient in the equation of state for cold seawater linearly relates density and temperature. The buoyancy forcing is therefore proportional to this coefficient, which due to the compressibility of seawater is a function of pressure, or equivalently depth. The thermobaric effect describes the dynamical impact of the variation of the thermal expansion coefficient with depth [Løyning and Weber, 1997].

The thermobaric effect is expected to cause colder fresher waters to become denser than warmer saline waters at depth [Killworth, 1977]. For this reason, sinking cold water acquires a negative buoyancy increase due to the thermobaric effect, which can overshadow positive buoyancy increases due to the differences in salinity. The depth dependence of density is most pronounced at low temperatures and in particular circumstances can provide an effective source of internal energy that accelerates the dense water current downslope, enhancing the dynamics of the outflow and possibly its down-slope penetration [Backhaus et al., 1997]. A cold dense outflow can become denser still relative to the ambient waters in a stably stratified ocean [Killworth, 1977]. At depths where the ambient water temperature approaches that of the cold dense flow, the thermobaric effect diminishes and normal dense overflow dynamics resume [Løyning and Weber, 1997]. The thermobaric effect is relatively unimportant except for very cold waters such as those formed in Arctic regions. For instance, the density contrast of the Filcher Ice Shelf outflow into Weddell Sea is due to its very cold temperature. The dependence of the density on pressure is highly

pronounced in the cold outflow and its descent through the weakly stratified warmer ocean waters is dominated by the thermobaric effect [Killworth, 1977]. In the Mediterranean, the outflow water is warm and saline and the thermobaric effect is reversed, retarding the descent of the flow through colder oceanic waters. However, as already mentioned, the effect is relatively small in comparison to the effects of entrainment and stratification in these warm waters [Backhaus et al., 1997].

In an investigation of the thermobaric effect [Jungclaus et al., 1995] the downslope propagation of a cold plume may be retarded by the thermobaric effect. The enhanced dynamics of the modelled cold plume also increase entrainment of the surrounding water masses, which generally acts to reduce the density contrast. In this particular case the cold plume also first entrains warm Atlantic Water, consequently becoming warmer than the ambient water mass below, Norwegian Sea Deep Water [Backhaus et al., 1997]. Model results such as this indicate that increased velocity of very cold sinking water due to the thermobaric effect may increase the downslope penetration of the plume, but the corresponding increase in turbulent entrainment acts to reduce it and the overall effect depends on the particular conditions [Jungclaus et al., 1995].

3.6. Seafloor topographic steering

The geostrophic flow is strongly influenced by irregularities in the local bathymetry and may be steered downslope by topographic features such as channels and canyons that cut the continental slope. These topographic constraints can alter the dynamical balance, increasing friction and reducing rotational effects [Killworth, 1977]. This can induce a geostrophically balanced downslope channel flow rather than predominantly alongslope flow with downslope flow in a viscous bottom boundary layer [Baines and Condie, 1998]. Dense fluid is directed downslope much more rapidly than a similar flow on a smooth slope [Lane-Serff, 2001]. Model simulations of topographic steering by realistic topography demonstrate how dense water slumping into a canyon could be steered downslope [e.g. Chapman and Gawarkiewicz, 1995]. In addition, the path of the Mediterranean outflow water, for example, is observed to be highly affected by topographic features and follow many depressions in the slope [Lane-Serff, 2001].

A simulation of a bottom arrested gravity plume on realistic topography [Backhaus et al., 1997] found that the flow splits at a topographic saddle point with part of the dense waters spreading northward towards the Fram Strait, in agreement with observations by Quadfasel et al. [1988]. Another branch of the flow is steered by topography into a deep trench east of the Knipovitch Ridge to the west of the Svalbard

continental slope [Jungclaus et al., 1995]. Although the existence of this branch remains to be confirmed by direct observations, Barents Sea water masses have been observed in that region.

Satellite altimeter measurements in combination with sparse measurements of seafloor depth currently provide the best available comprehensive map of seafloor topography on scales greater than about 10km [Baines and Condie, 1998]. However, there is much evidence of topographic features on scales less than 10km on continental slopes. Submarine canyons, for example, typically have relatively steep sides and widths of several kilometres and the continental slope of Antarctica is believed to be full of topographic features of this scale. As discussed above, these features are important to the dynamics of dense water overflows and cascades, but are currently inadequately known.

3.7. Density and volume properties of the outflow

The resulting product waters that finally disperse into the ocean interior often have quite different characteristics from the source waters outflowing at the top of the continental slope. For example, the Mediterranean Sea outflow source water is considerably denser than that of the Denmark Strait outflow, but produces only intermediate depth waters [Price, 1994]. The final product water is determined not only by the density of the source water at the top of the slope, but also by effects and processes that modify the density and volume properties of the dense water on its descent, such as entrainment and detrainment [Legg et al., 2004].

As outflows descend, they entrain ambient water along their path due to turbulent cross frontal shear instability (e.g. Condie, 1995). The overlying lighter water mixes with the dense outflow water, decreasing its density and momentum, and increasing its volume significantly [Baines and Condie, 1998; Hill et al. 1998]. The density contrast between the dense outflow and the ambient water is therefore reduced, constraining its ability to sink into the deep sea [Schauer and Fahrbach, 1999].

Numerical investigations by Price [1994] found that the density of the product water is insensitive to variations in the source water density. Increased density of the source water also increases the density contrast with the ambient water. In turn, the speed of the density driven geostrophic flow is larger resulting in more vigorous entrainment. Increased entrainment of the ambient water, which is relatively even lighter in comparison to the dense bottom water, acts to eradicate much of the imposed source density increase. This insensitivity to variations of the source water density is therefore due to a strong damping of density contrasts by corresponding changes in the entrainment rate [Shapiro et al., 2003]. For

example, the even more vigorous entrainment resulting from arbitrarily increasing the density of the model Mediterranean source water by 1 kg m^{-3} increases the transport of product water by about 10^6 m^3 s^{-1} and limits the increase in density of the product water to only about 0.15 kg m^{-3} [Price, 1994], indicating that entrainment is a crucial component of abyssal water production.

In addition, entrainment mixes substantial volumes of ambient water into the dense overflow. Quadfasel et al. (1988), for example, estimated from observations of the dense outflow from Storfjord, Svalbard into the Norwegian Sea, one of the few observed cases of slope convection in the Arctic, a volume increase due to entrainment of around 500% [Backhaus et al., 1997]. The final outflow density is therefore considerably more sensitive to variations in the density of the ambient water.

These results indicate that the mixing with the ambient oceanic waters and its properties, are of considerable importance in determining the properties of the product water and thus the depth of the overturning circulation [Price, 1994]. This is supported by model simulations for the North Atlantic circulation where the modelled thermohaline circulation is strongly dictated by the details of mixing of the North Atlantic overflows [Willebrand et al. 2001; Özgökmen and Chassignet, 2002].

3.8. Entrainment and the ambient water

The rate of entrainment and its effect does vary substantially between outflows. An important feature of the entrainment process is that it is quite localised and shallow in depth with the intensity of mixing varying along the path of the outflow. In this respect, entrainment is quite different from diffusion processes that act homogenously. Indeed, increased entrainment rates are considered to be related to increased topographic slopes [Girton and Sanford, 2003]. For example, during the descent of the Faroe Bank Channel outflow, strong entrainment usually occurs over short sections of the path where bottom topography is steepest [Price, 1994].

In high latitude outflows, entrainment typically results in a much lower density decrease mainly due to the lower density difference between the overflow and the ambient waters. For example, as the Mediterranean Sea outflow descends the continental slope, strong entrainment of North Atlantic water decreases its density by about 1 kg m^{-3}, whereas the rate of density decrease of the Denmark strait and Weddell Sea outflows due to entrainment is much less with average values of 0.1 kg m^{-3} and 0.03 kg m^{-3} respectively [Price, 1994].

Many dense bottom outflows entrain a number of different ambient water masses during their descent, leading to distinct product water characteristics. For instance, the ambient waters entrained by the dense outflow from Storfjord, Svalbard include East Spitsbergen shelf water, Atlantic water and Norwegian Sea deep water [Quadfasel et al., 1988; Schauer, 1995]. Realistic simulations of overflows must therefore incorporate the density properties of a number of overlying water masses and their mixing accurately.

Entrainment of overlying seawater during the descent of dense bottom flows has a number of important roles in their downslope propagation. Without entrainment, the downslope propagation of down slope front (of the dense outflow) is severely constrained by friction. Friction restricts the supply of dense water from the flow behind to the downslope front, which is needed to force density-driven propagation of the outflow. Turbulent entrainment thickens the downslope front, allowing a greater supply of dense water to the downslope front and so increasing the downslope speed of the outflow [Shapiro et al., 2003]. Also, the entraining outflow transfers ambient water mass properties to depth. For example, a cold and saline plume entraining warm and saltier ambient waters may achieve a net downward transport of heat and salt in the ocean waters [Ivanov et al., 2004; Backhaus et al., 1997]. This is in contrast to open ocean convection, which usually accounts for an upward transport of heat and salt, as occurs in the Greenland Sea for example [Rudels and Quadfasel, 1991].

3.9. Detrainment and the ambient water

The overflow generally descends through a stably stratified oceanic environment. Numerical models of overflows demonstrate the important effect of ambient stratification on the propagation of the outflow. The density contrast between the overflow and the stratified ambient water decreases with depth, as the density of the stratified water increases with depth. Jiang and Garwood [1998] found that as well as this direct effect, in a stratified environment the density contrast further decreases due to enhanced mixing. The descent of an overflow is therefore impeded by ambient stratification and as such the down slope penetration is greater for weak stratification. High latitude outflows are therefore more likely to reach the bottom as the oceanic water column in polar and subpolar seas is typically weakly stratified, such as in Weddell Sea [Price, 1994].

Laboratory experiments [e.g. Lane-Serff and Baines, 1998] show that in a stratified environment such as that of the ocean, and for sufficiently shallow slope angles comparable with those of the continental slope, fluid detrains from the dense plume over most of its length. These experiments were conducted in non-

rotating environments. However, their existence in the ocean is implied by observations, and other experiments show that the effects are also present in rotating fluids, although they remain to be quantified.

Fluid nearer the density front of the overflow is not fully mixed with fluid closer to the bottom and small-scale turbulent mixing processes at the density front [Baines and Condie, 1998], or possibly strong changes in direction of the flow due to local bathymetry [Lane-Serff, 2001], may cause some of this fluid to leave the main plume [Baines and Condie, 1998]. Any mixed fluid formed at the density front in a homogenous environment is still denser than the ambient water and therefore eventually rejoins the dense bottom flow. With a stratified environment, the density of the mixed fluid may equal that of the ambient water at shallower depths than the final depth reached by the main flow. The mixed fluid may thus be shed from the overflow at its own density level [Lane-Serff, 2001] and some dense shelf or marginal sea water therefore enters the ambient ocean over a broad range of depths [Baines and Condie, 1998]. The detrained fluid may form eddies [Etling et al., 2000] or domes of rotating dense water [Lane-Serff, 2001]. Relatively well mixed domes of fluid have been observed downstream of the Mediterranean Sea outflow, which propagate around the North Atlantic for substantial amounts of time.

3.10. Sediment

Model investigations on the influence of suspended sediments in bottom gravity flows indicate their possibly significant role in enhancing cascading and hence water mass formation [Backhaus et al., 1997]. This is substantiated by geological data [Fohrmann, 1996 in Backhaus et al., 1997]. Sediments may be initially dispersed in sufficiently strong bottom gravity flows, or eroded during its descent thereby increasing the density of the flow due to the extra weight of suspended particles [Backhaus et al., 1997 and Baines and Condie, 1998]. The flow forms a turbidity current with suspended sediments increasing the density and therefore the negative buoyancy of the bottom gravity plume. This enhances the dynamics of the plume and is expected to result in stronger and more direct downslope flows [Baines and Condie, 1998; Backhaus et al., 1997]. Suspended sediments may therefore amplify the transport of dense surface waters by slope convection.

The sediment laden bottom plume descends until reaching a depth where its own density is equal to that of the ambient seawater where it leaves the slope as an intrusion into the ocean interior. Here the flow slows and weakened turbulence allows the sediments to be deposited as demonstrated schematically in Figure 3.3. This may lead to significant lightening of the intrusion initiating its ascent and upward convection in

the ambient ocean. The final depth of a sediment-laden outflow is not therefore necessarily dependent on its enhanced density due to the suspended sediments.

Figure 3.3. Schematic of the isopycnal intrusion of a sediment-laden gravity plume from sloping topography. Settling of sediments causes upward directed internal convection [reproduced from Backhaus et al., 1997].

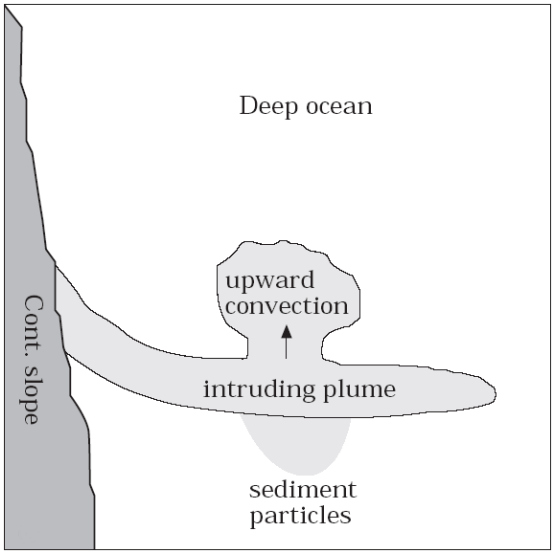

Sediment deposition at the base and lower areas of the continental slope, such as that in the Ross Sea, or high concentrations of suspended sediment in abyssal layers close to the base of the continental slope provide evidence of the occurrence of this phenomenon [Backhaus et al., 1997]. However, it is unknown whether sediment processes in dense overflows are continuous or large transient occurrences [Baines and Condie, 1998]. Sediment transports are sensitive to extremes of currents. An 18-year record of the Santa Clara River, USA, for example, showed 60% of the sediment transport occurring in just six days [Huthnance, 1995], which also highlights the sampling problem for measurements. The possible role of sediments in the descent of dense water overflows and cascades, and deep water mass formation has not been studied in much detail yet. However, numerical investigations by Kampf and Fohrmann [2000] demonstrated the importance of sediment plumes in triggering deep water renewal and found them to be intermittent features.

3.11. Equilibrium density level

The cascading dense bottom flow eventually reaches a level where its density is equal to that of the ambient ocean water [Shapiro et al., 2003; Lane-Serff, 2001]. This depth of this level depends on the

initial source water properties and crucially on the properties of ambient water and the amount that is entrained into the overflow, as already discussed in this chapter. The descended water detaches from the continental slope at its equilibrium density level and spreads isopycnally into the ambient waters of the deep ocean. This intrusion may be at intermediate or deep levels, or if the density excess of the cascading flow remains at the foot of the slope, the descended dense water may spread over the ocean floor and become the bottom water mass. In many cases temperature and salinity contrasts remain and the intrusion continues to evolve, exchanging heat and salt in order to assimilate itself with the surrounding water [Ivanov et al., 1997]. Diffusion is now expected to be the most efficient mechanism controlling this process, although it may be assisted by irregularities in the ocean floor. Strong ambient currents may also facilitate the spreading the overflow origin water away from the vicinity of the slope [Shapiro et al., 2003].

3.12. Summary

A dense bottom flow descends under a balance of gravity, the Earth's rotation, bottom friction and turbulent entrainment. On the sloping bathymetry the influence of gravity increases flow velocity and thus friction and the contribution of ageostrophic effects. These effects allow a downslope component of flow, in addition to the predominantly geostrophic alongslope flow, and downslope drainage in the viscous bottom boundary layer. Cascading is primarily related to the geostrophic along slope flow. However, the weaker the rate of source water production, the greater the contribution of bottom friction to the source balance. In addition, instability of a thick broad dense bottom flow may generate strong eddies. Their generation is suppressed for a moderate flow and a weak flow is viscously controlled.

Entrainment and detrainment decrease the density of the bottom gravity current, with entrainment also substantially increasing the volume of the flow. The degree of entrainment and detrainment depends on the velocity of the flow, the initial density of the bottom current and the thermohaline properties of the ambient water. The thermobaric effect, topographic features and suspended sediments may all enhance the dynamics of the overflow and increase its downslope velocity. However, the overall effect on the final depth reached by the dense overflow depends in the particular conditions due to the associated increase in entrainment and detrainment. Downslope penetration is greater for weakly stratified ambient water. The product water has quite different volume and density properties to the source water and is insensitive to variations of the source water density due to a strong damping by corresponding changes in the rate of entrainment. Instead it largely depends on the thermohaline properties of the ambient water and the rate of its entrainment.

Chapter 4

Simple Plume Model

4.1. Introduction

In order to realistically reproduce overflow dynamics, it is necessary to account for all major processes involved. However, much simpler models allow us to isolate and gain insight into the underlying physical mechanisms. A simplified *process* model is useful for analysing outflow dynamics and for examining specific cascading mechanisms. For example, a process model can be used to estimate the sensitivity of the outflows to variations of mixing, or density of the source water.

In the present study a simple plume model is used to assess the role of bottom topography and friction in determining the path, the rate of descent, and the evolution of the thickness and width of the outflow. The effect on a model outflow of constant, concave, convex and corrugated slope bathymetry is investigated. In each scenario the average gradient of the slope is unchanged from that of the constant slope. We test the hypothesis that the presence of steeper areas allows the flow to descend faster, despite the maintenance of an average gradient. We therefore expect the outflow to descend more quickly over corrugated, concave and convex bathymetry than over the constant slope.

4.2. The model

A plume model for the dense overflow is a steady flow on a simple slope as demonstrated in Figure 4.1. It is assumed that the outflow can be represented by a single layer and the oceanic environment is effectively infinite and at rest with

$$h << H$$

where h is the vertical thickness of the dense layer and H is the depth of the topography from the sea surface. Within this layer the density has a uniform value $\rho_0 + \Delta\rho$, where ρ_0 is the density of the unstratified ambient fluid. Flow is confined to this bottom layer, and is thus described by reduced gravity dynamics. We assume the hydrostatic approximation, which is valid when horizontal motions are very large compared to vertical motions such as those of an overflow. The pressure at the top of the bottom layer can therefore be written as:

$$p = -\rho_0 g'(H - h)$$

where

$$g' = \frac{g\Delta\rho}{\rho_0}$$

is the reduced gravity. Friction on the ocean bottom is parameterised by a linear drag with drag coefficient r. The overflow is assumed to be flowing geostrophically to leading order and an f-plane approximation is assumed for simplicity. The dense and ambient layers are assumed to be well mixed with uniform density. The outflow is assumed to be steady, which is probably valid on longer timescales, and strong mixing processes, although an integral part of density current dynamics, are ignored due to time constraints on this study.

Figure 4.1. Schematic of the plume model.
The horizontal velocity is given by $\underline{u}$, ρ_0 is the density of the ambient water, $\Delta\rho$ is the density excess, h is the vertical thickness of the dense layer and H is the depth of the topography from the sea surface.

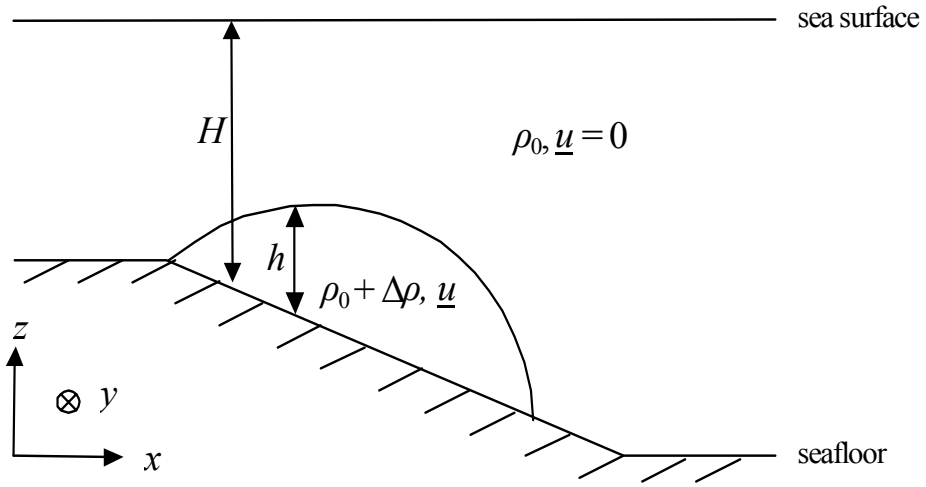

The equations of motion for this model are therefore the momentum equation

$$f\underline{k}\times\underline{u}-g'\nabla\left(H-h\right)=-r\underline{u} \tag{1}$$

and the continuity equation

$$\frac{\partial h}{\partial t}+\nabla.\left(h\underline{u}\right)=0\,. \tag{2}$$

4.3. Derivation of a single equation in *h*

We can now form a single equation for *h* taking $\underline{k}\times$ (1) we obtain

$$-r\underline{u}=\frac{rg'}{f}\underline{k}\times\nabla(H-h)-\frac{r^2}{f}\left(\underline{k}\times\underline{u}\right).$$

Substituting (1) in the left hand side gives

$$f\underline{k}\times\underline{u}-g'\nabla\left(H-h\right)=\frac{rg'}{f}\underline{k}\times\nabla(H-h)-\frac{r^2}{f}\left(\underline{k}\times\underline{u}\right)$$

$$f\left(1+\frac{r^2}{f^2}\right)\underline{k}\times\underline{u}-g'\nabla\left(H-h\right)=\frac{rg'}{f}\underline{k}\times\nabla(H-h)\,.$$

Now $\frac{r^2}{f^2}<<1$ so neglecting this term and multiplying by *h* gives

$$h\underline{u}\approx\frac{rg'}{f^2}h\nabla(H-h)-\frac{g'}{f}h\underline{k}\times\nabla(H-h)\,. \tag{3}$$

Substituting (3) into (2) gives

$$\frac{\partial h}{\partial t}+\nabla h.\left(\frac{rg'}{f^2}\nabla H-\frac{g'}{f}\underline{k}\times\nabla H\right)\approx-\frac{rg'}{f^2}h\nabla^2H+\frac{rg'}{f^2}\nabla.h\nabla h\,. \tag{4}$$

This is a single equation in one unknown, *h*.

4.4. Method of solution

Equation (4) can be rewritten as

$$\frac{\partial h}{\partial t}+\underline{u}_c.\nabla h\approx-\frac{rg'}{f^2}h\nabla^2H+\frac{rg'}{f^2}\nabla.h\nabla h \tag{5}$$

where

$$\underline{u}_c = \frac{rg'}{f^2}\nabla H - \frac{g'}{f}\underline{k}\times\nabla H = \left(\frac{rg'}{f^2}\frac{\partial H}{\partial x} + \frac{g'}{f}\frac{\partial H}{\partial y}, \frac{rg'}{f^2}\frac{\partial H}{\partial y} - \frac{g'}{f}\frac{\partial H}{\partial x}\right)$$

is the characteristic velocity. The *x*-axis is directed horizontally eastwards, the *y*-axis is directed northwards alongslope and the *z*-axis is directed upwards as indicated in Figure 4.1. For $r << f$ the characteristic velocity is directed at an approximately fixed angle to the bathymetric contours where the angle of descent is $\frac{r}{f}$. The second term on the right hand side of (5) is diffusive, but generally small.

Assuming the width of the current is far less than the characteristic length scale along the current, (5) can be approximated by

$$\frac{D_c h}{Dt} \approx -\frac{rg'}{f^2}h\left(\frac{\partial^2 H}{\partial x^2}\right) + \frac{rg'}{f^2}\frac{\partial}{\partial x}\left(h\frac{\partial h}{\partial x}\right) \tag{6}$$

where

$$\frac{D_c}{Dt} = \frac{\partial}{\partial t} + \underline{u}_c.\nabla .$$

We can now solve for *h* numerically by the method of characteristics. The characteristic velocity is known as it depends only on the prescribed bathymetry. Information propagates downstream along the characteristics and the equation can be stepped forward in time from the initial conditions, which are the starting position and the initial values of height and width of the outflow.

Integrating the model equation (6) using a forward time step gives

$$h\left(\underline{x} + \underline{u}_c\Delta t, t + \Delta t\right) \approx h\left(\underline{x}, t\right) - \Delta t\frac{rg'}{f^2}\left(h\left(\frac{\partial^2 H}{\partial x^2}\right) - \frac{\partial}{\partial x}\left(h\frac{\partial h}{\partial x}\right)\right). \tag{7}$$

A flux method is used for the third term on the right hand side in order to conserve fluid giving

$$h^{n+1}\left(\underline{x} + \underline{u}_c\Delta t, t + \Delta t\right) \approx h_{ij}^n\left(\underline{x}, t\right) - \Delta t\frac{rg'}{f^2}\left(h_{ij}^n\left(\frac{\partial^2 H}{\partial x^2}\right) - \frac{1}{\Delta x_1 + \Delta x_2}\left(\frac{{h_{i+1j}^n}^2 - {h_{ij}^n}^2}{\Delta x_2} - \frac{{h_{ij}^n}^2 - {h_{i-1j}^n}^2}{\Delta x_1}\right)\right)$$

(8)

Note, the second term on the right hand side is not written in conservative form and a forward step discretisation is not an optimal choice. Given more time, a range of schemes would have been investigated, such as Runge-Kutta. In addition, although the scheme is numerically convergent, comprehensive convergence testing has not been undertaken due to time restrictions.

4.5. Boundary conditions

The initial condition of the outflow is a parabola with an approximate width, w_0, of 50 km and thickness at the vertex, h_0, of 150 m as indicated in Figure 4.2. Marginal sea outflows are thin, having aspect ratios in the range 0.001 < depth/width < 0.01 [Price, 1994] and the initial condition is based on the values used in Price and Baringer [1994] to model the Denmark Strait Overflow. The exact value used is altered slightly depending on the bathymetry in order to preserve the initial area of the outflow. The flow is started at time $t = 0$ and position $0 \leq x \leq w_0 \cos\theta$, $y = 0$. The depth H_0 below the sea surface is reference depth at $z = 0$ from which the depth of the outflow is measured as indicated in Figure 4.2. The continental slope descends at an average angle in excess of 4° [Continental slope, Encyclopædia Britannica, n.d.] and the slope angle θ was consequently set to 0.07 radians (~ 4°). The drag coefficient, $r = 5 \times 10^{-6}$ s^{-1} unless otherwise stated and the other parameters are taken to be $g' = 0.01$ ms^{-2}, $f = 10^{-4}$ s^{-1}, $\Delta t = 1000$ s.

Figure 4.2. The initial conditions.
The initial thickness of the outflow at the vertex is h_0, w_0 gives the initial width of the outflow, H_0 is a horizontal datum level at $z = 0$ and θ is the angle between the sloping topography and the horizontal.

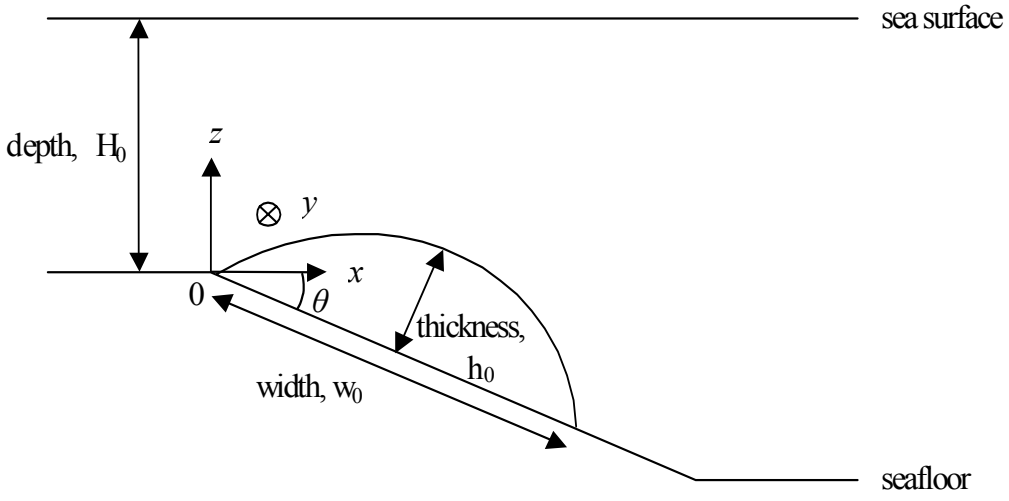

4.6. Choice of bathymetry

A number of forms of bathymetry are considered in order to investigate the effect of steep slope regions on the descent of a dense plume.

(a) Constant slope

In the first numerical experiment, the bottom topography is represented by a plane as illustrated in Figure 4.3, where

$$\frac{dH}{dx} = \tan\theta ,$$

$$\frac{dH}{dy} = 0$$

and $\nabla^2 H = 0$.

(b) Concave slope

A parabola about the constant slope represents the concave bottom topography, as illustrated in Figure 4.4. The topography varies only in the *x* direction and hence

$$\frac{dH}{dy} = 0 .$$

The height and width of the bathymetry parabola are given similarly to the initial condition of the outflow as illustrated in Figure 4.2. The height is the perpendicular distance of the vertex from the constant slope, and the width is the distance, parallel to the constant slope, between where the parabola intersects the constant slope.

(c) Convex slope

A parabola about the constant slope represents the convex bottom topography, as illustrated in Figure 4.5. The topography varies only in the *x* direction and hence

$$\frac{dH}{dy} = 0 .$$

The height and width of the bathymetry parabola are given similarly to the concave bathymetry.

(d) Corrugated slope

A corrugation (oscillation) of the bottom topography in the *y* direction around the constant slope, as illustrated in Figure 4.6, is represented by the addition of a second term on the right hand side.

$$\frac{dH}{dx} = \tan\theta + a\sin(ky)$$

and $$\frac{d^2H}{dx^2} = 0$$

where a is the amplitude of the corrugation and k is the period. Integrating we obtain

$$H = x\tan\theta + ax\sin(ky) + \mathrm{H}_0$$

Therefore

$$\frac{dH}{dy} = akx\cos(ky)$$

$$\frac{d^2H}{dy^2} = -ak^2x\sin(ky)\,.$$

Figure 4.3. The model constant slope bathymetry. The bathymetry shown is calculated along 59 characteristics in total, where characteristics 11 to 49 capture the initial outflow. The left and right edges of the shaded region follow characteristics 1 and 59. The remaining characteristics are parallel to and between these. The colour scale is the depth in metres below H_0.

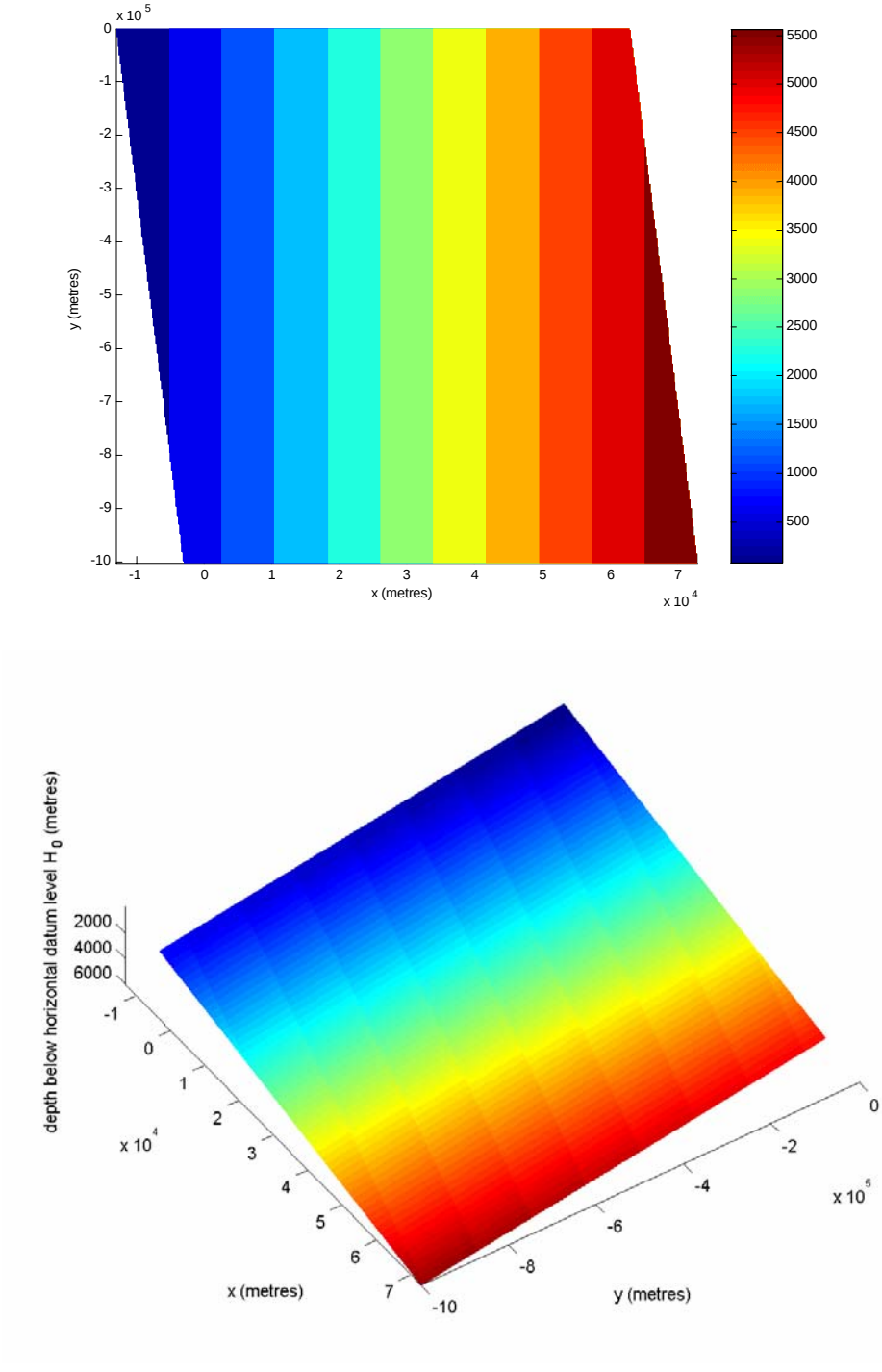

Figure 4.4. The model concave slope bathymetry. The bathymetry shown is calculated along 59 characteristics in total, where characteristics 11 to 49 capture the initial outflow. The left and right edges of the shaded region follow characteristics 1 and 59. The remaining characteristics are between these and converge with increasing *y* although this is not clearly visible in this case. The colour scale is the depth in metres below H_0.

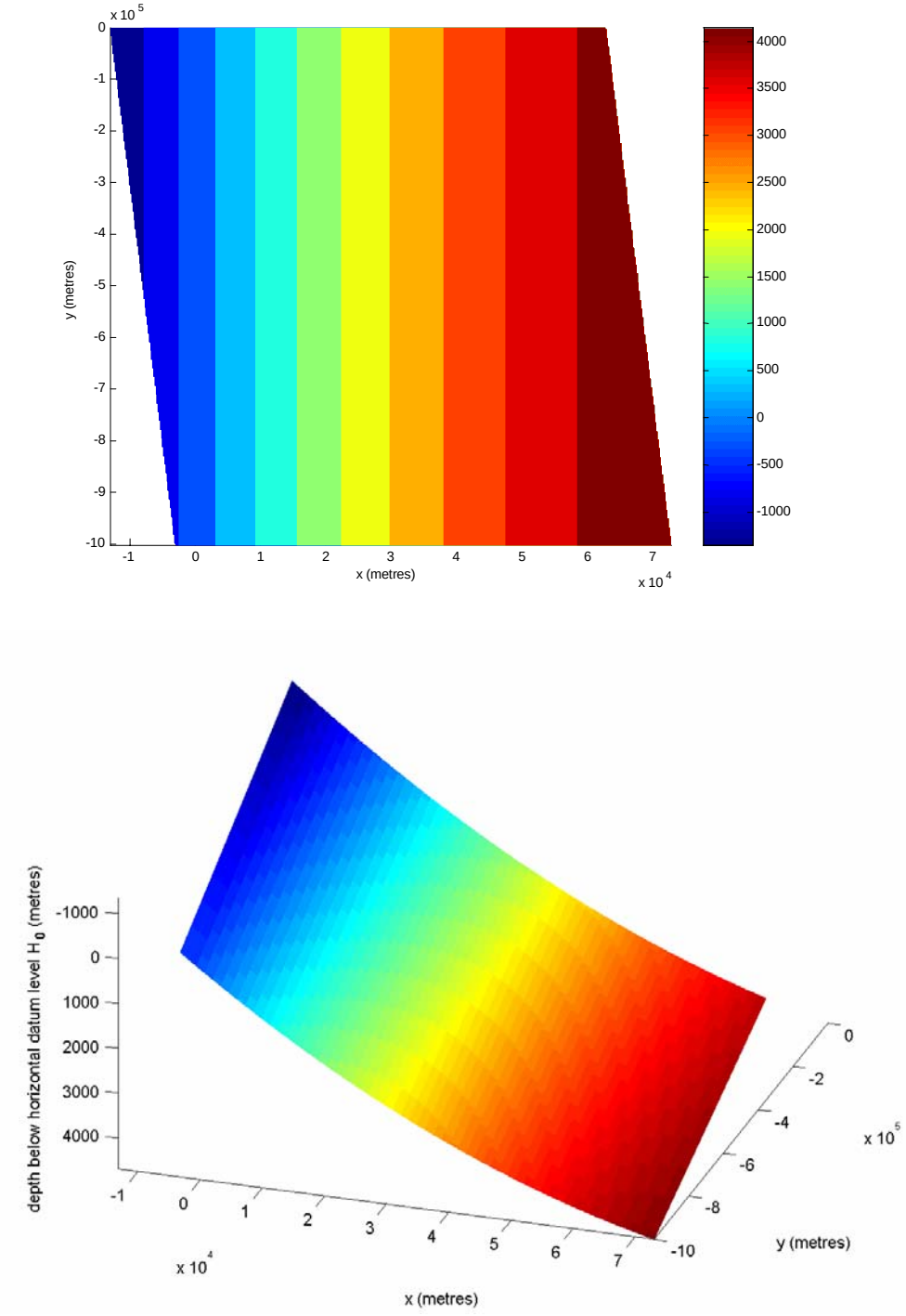

Figure 4.5. The model convex slope bathymetry. The bathymetry shown is calculated along 59 characteristics in total, where characteristics 11 to 49 capture the initial outflow. The left and right edges of the shaded region follow characteristics 1 and 59. The remaining characteristics are between these and diverge with increasing y although this is not clearly visible in this case. The colour scale is the depth in metres below H_0.

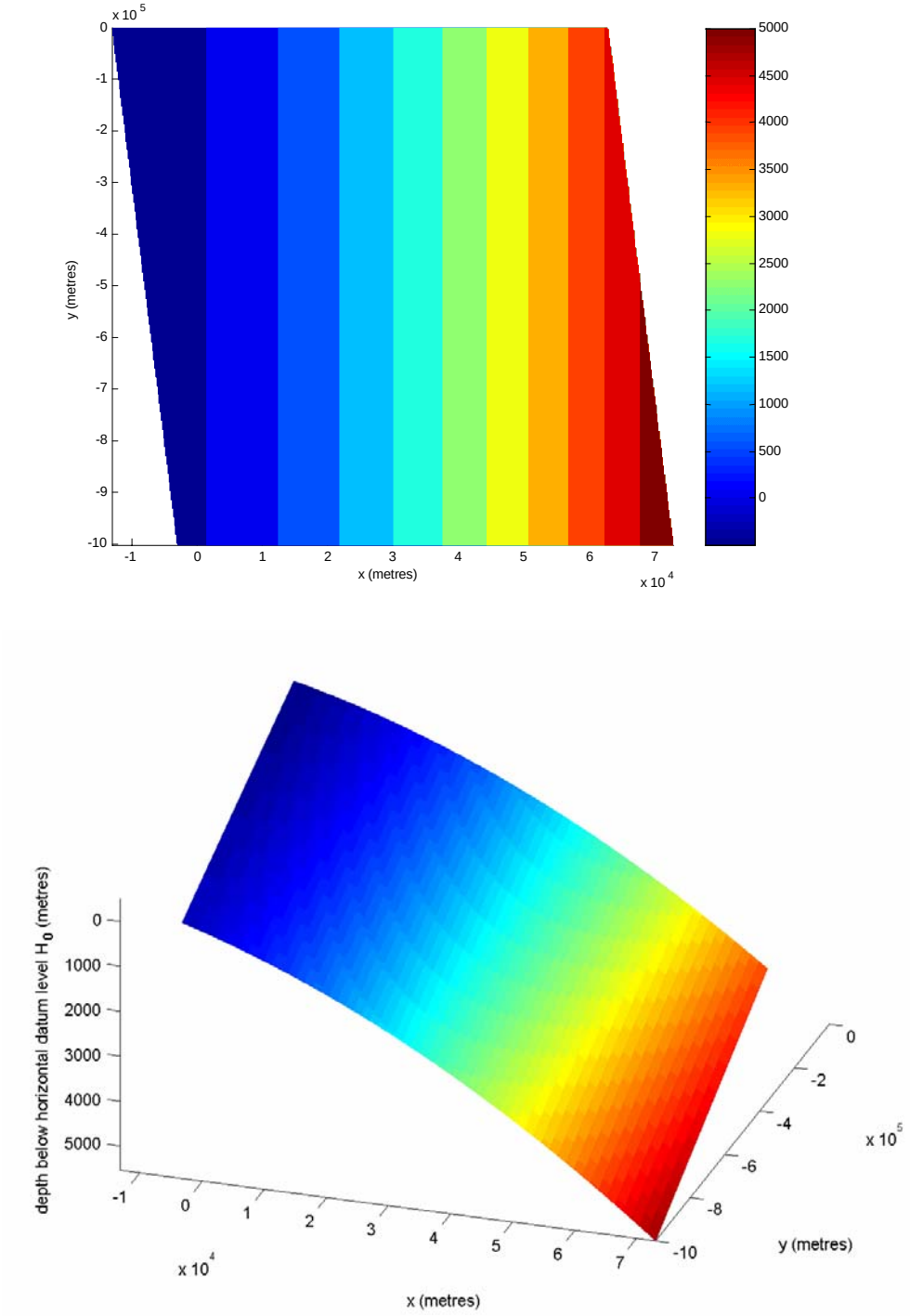

Figure 4.6. The model corrugated slope bathymetry. The bathymetry shown is calculated along 59 characteristics in total, where characteristics 11 to 49 capture the initial outflow. The left and right edges of the shaded region follow characteristics 1 and 59, with the remaining characteristics between these. The colour scale is the depth in metres below H_0. The amplitude, a, of the corrugation is given as a function of x in the vertical plane. In this case $a = -0.03x$ m. For $a < 0$, the corrugation is initially approaching a trough and for $a > 0$, the corrugation is initially approaching a ridge.

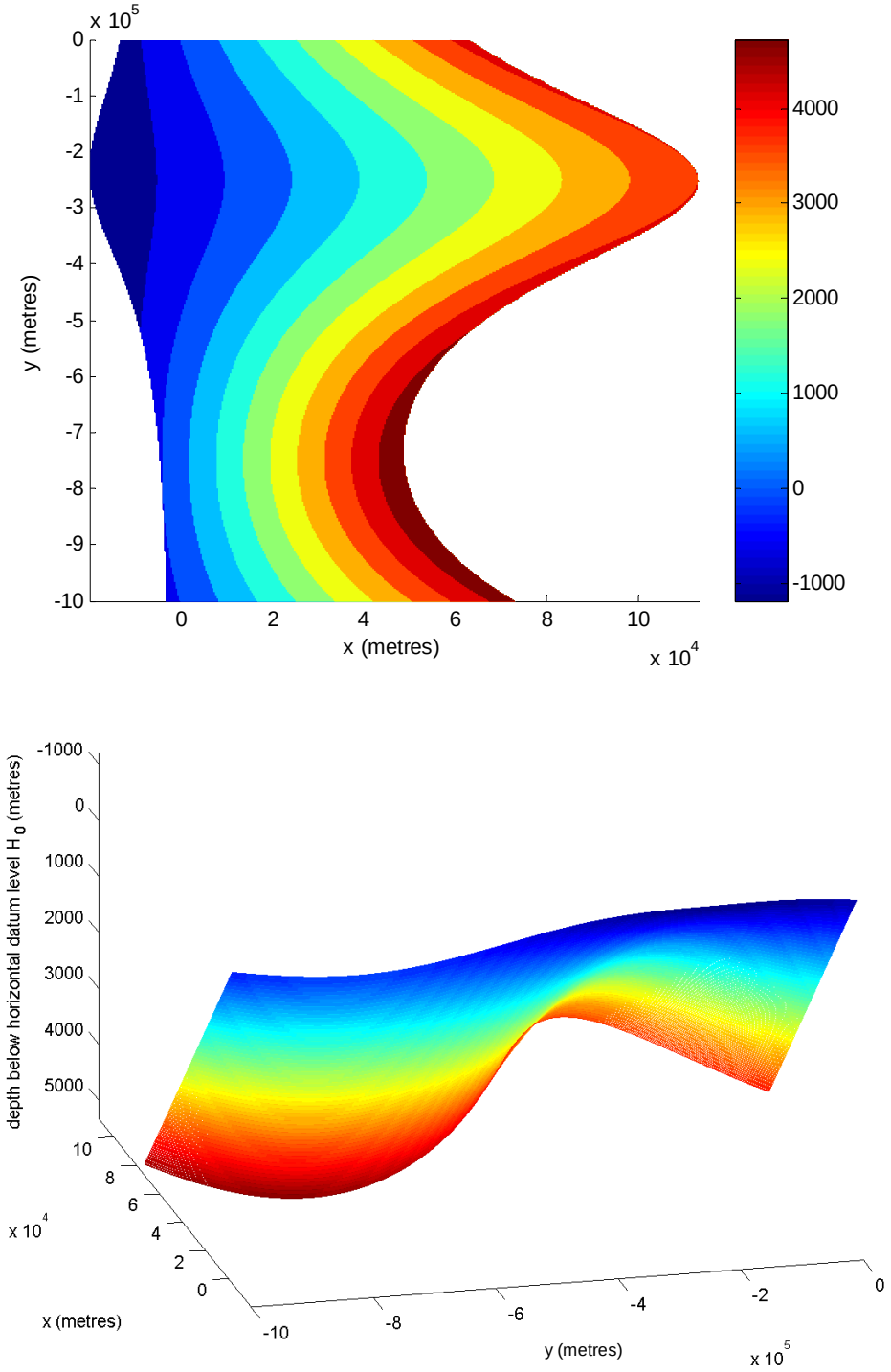

4.7. Results: Path of the flow

Once initialised, only the characteristic velocity and therefore the bottom topography determine the path of the flow along the characteristics. In this section we examine and compare the rates of descent along the characteristics for each of the four different bottom topographies. Although outflows can flow for hundreds of kilometres downstream, the cross slope angle in large outflows is quite small. For the convex and concave cases the topography varies only in the across stream (x) direction. In order to emphasize any effects of the topography, the friction is taken to be the slightly inflated value of 5×10^{-6} s^{-1} in order to increase the cross slope angle, and the model is allowed to run for much longer than is realistic. The convex and concave bathymetries are taken to have a width of 60 km, and heights of 400 m and – 400 m respectively. The amplitude of the corrugated bathymetry is taken to be 0.03 x and the number of periods of the corrugation is one, unless specified otherwise.

The path along a characteristic is given by

$$\underline{x}^{n+1} = \underline{x}^{n} + \underline{u}_c{}^{n} \Delta t$$

and $$t^{n+1} = t^{n} + \Delta t \, .$$

The downslope propagation of the characteristics with constant, concave, convex and corrugated slope topography is compared and the results are shown in Figure 4.7. The initial data is advected with the characteristic speed. For the constant slope topography, the characteristic speed is also constant and the characteristics are parallel straight lines (Figure 4.7(a)). In the other cases, the steepness of the topography is variable across the outflow and the characteristic speed, which depends only on the topography, is not constant. The characteristics are distorted, converging for concave bathymetry (Figure 4.7(b)), and diverging for convex bathymetry (Figure 4.7(c)). For corrugated topography, it is evident by a comparison between Figures 4.7(d) and 4.8 that the across slope gradient controls the downslope propagation of the flow. In the across slope direction the characteristics diverge in flatter regions (i.e. over a ridge) and converge in steeper regions (i.e. in a trough), subsequently returning to their initial distribution after each period of corrugation (Figure 4.8). In the along slope direction, the characteristics appear to maintain their initial distribution with time (Figure 4.7(d)) and although there is a slight variation this is overshadowed by the across slope flow.

A comparison of the characteristic depth reached with time between the four different bottom topographies, shown in Figure 4.9, does not demonstrate that steeper regions allow the overflow to descend more quickly when an average gradient is maintained. Instead the flow along the characteristics

takes longer to descend. This is most likely due to the overall greater distance travelled over the curved bathymetry, which can be inferred from Figures 4.10 and 4.11. The characteristics for corrugated bathymetry converge to those for constant bathymetry as the amplitude of the corrugation decreases, which also decreases the overall distance travelled (Figure 4.10). When the period of the corrugation is halved, this does not affect the overall distance travelled and the time taken does not alter as illustrated in Figure 4.11.

Figure 4.7. The downslope propagation of the characteristics with (a) constant slope bathymetry. (b) concave slope bathymetry. (c) convex slope bathymetry (d) corrugated slope bathymetry. In all cases, the average gradient of the slope is equal to that of the constant slope, tan θ.

(a)

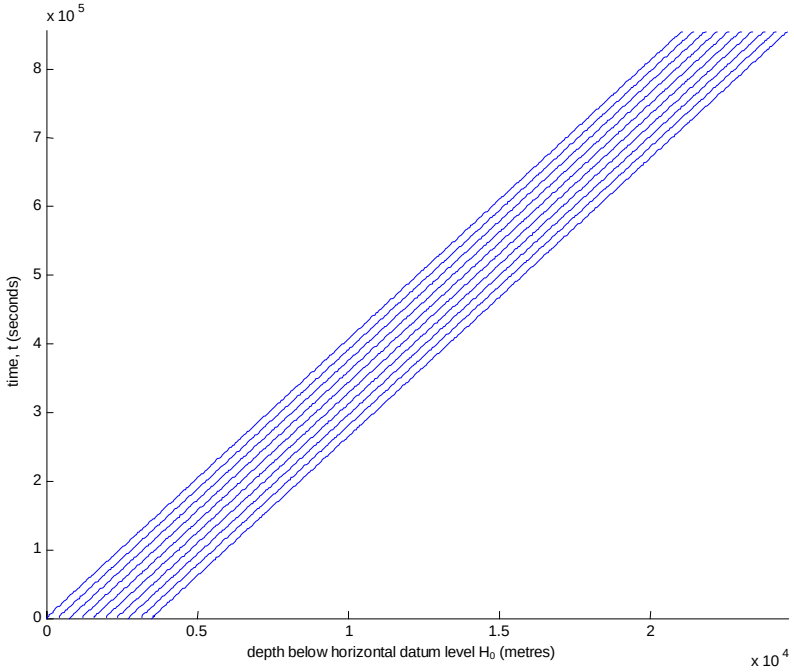

(b)

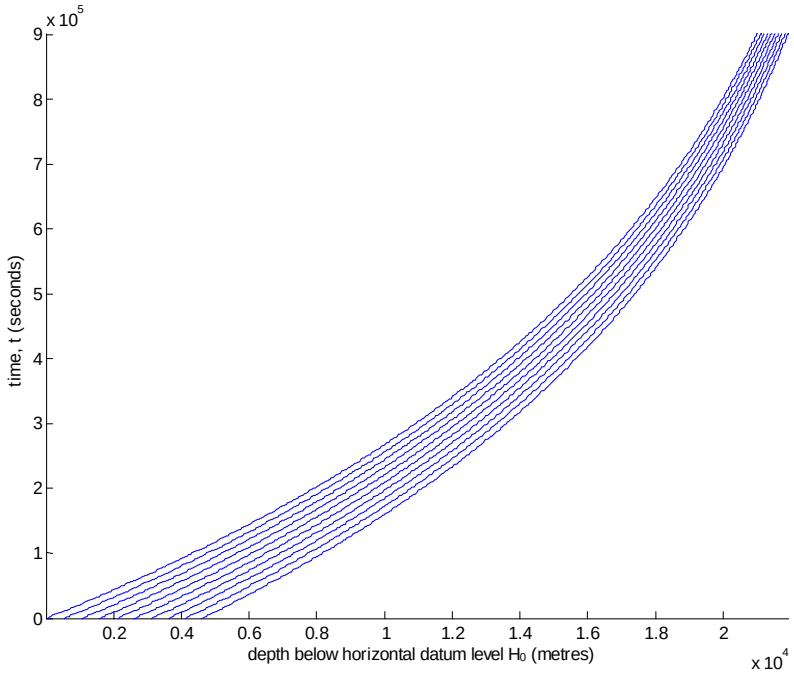

(c)

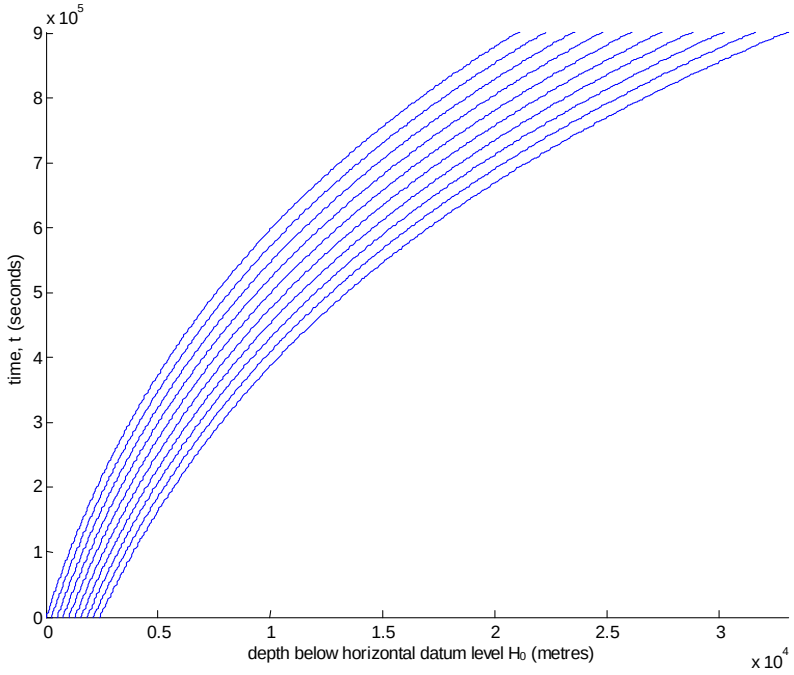
x 10^5
9
8
7
6
5
4
3
2
1
0
time, t (seconds)
0
0.5
1
1.5
2
2.5
3
depth below horizontal datum level H0 (metres)
x 10^4

(d)

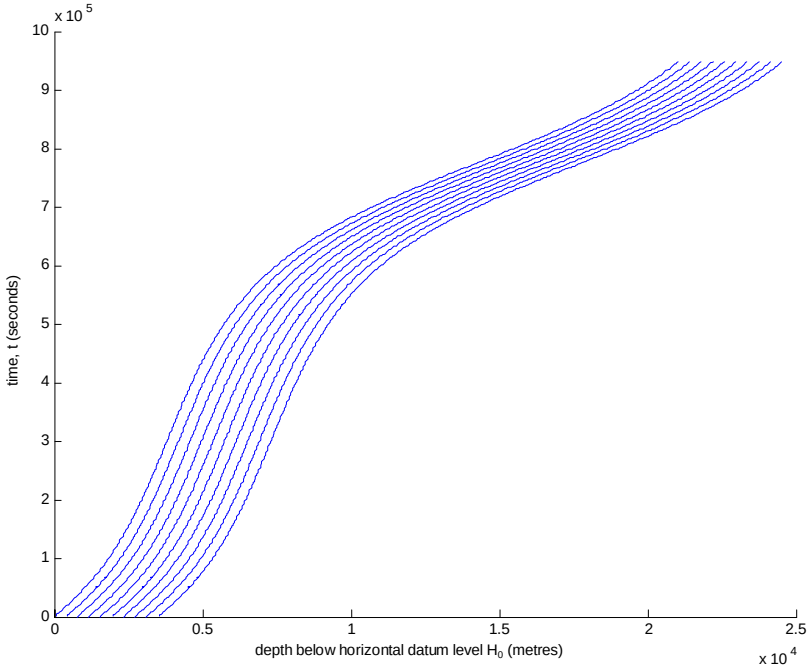
x 10^5
10
9
8
7
6
5
4
3
2
1
0
time, t (seconds)
0
0.5
1
1.5
2
2.5
depth below horizontal datum level H0 (metres)
x 10^4

Figure 4.8. The across slope propagation of the characteristics with corrugated slope bathymetry.

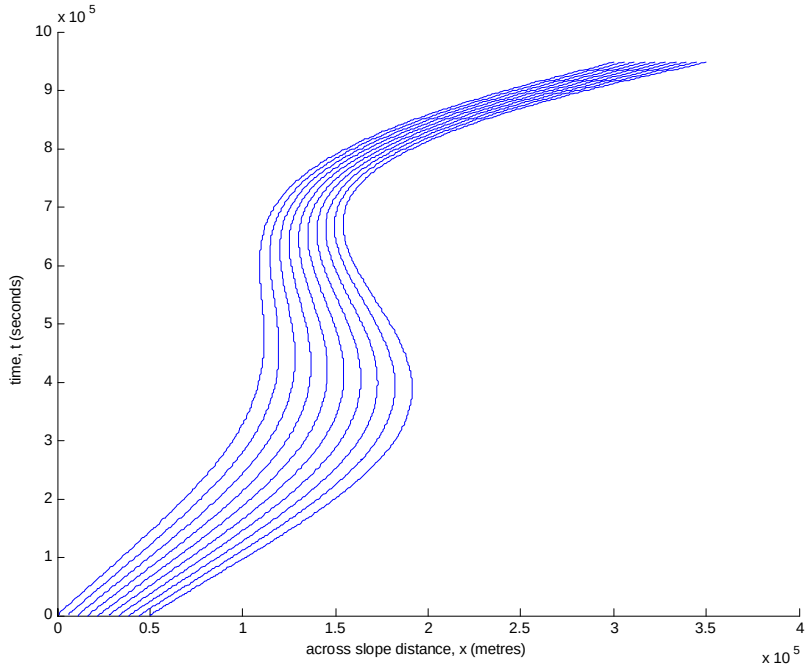

Figure 4.9. Comparison between the times taken to reach depth level along a characteristic for the four different bathymetries. The characteristic is initially at $x = y = 0$.

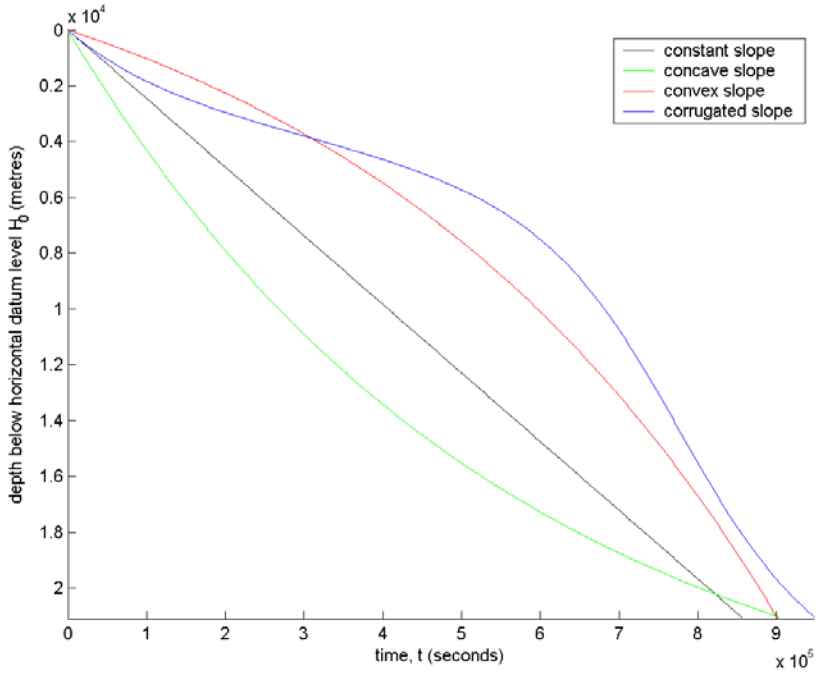

Figure 4.10. Comparison of the times taken along a characteristic to reach a depth level over one period of the corrugation with varying amplitude of the corrugation. The characteristic is initially at $x = y = 0$.

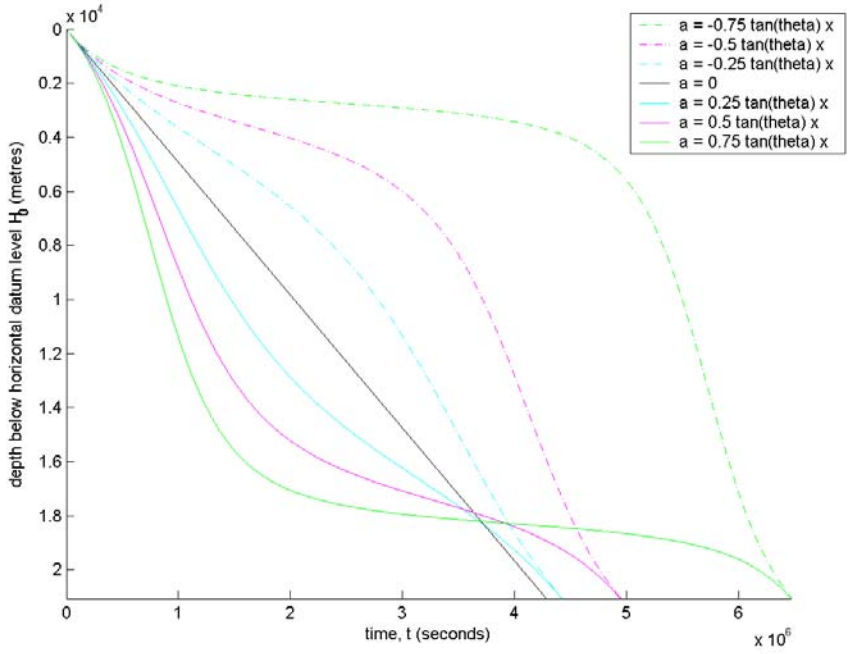

Figure 4.11. Comparison of the times taken along a characteristic to reach a depth level with varying periods of the corrugation. The characteristic is initially at $x = y = 0$. The number of periods of the corrugation, n, is specified. The amplitude of the corrugation is 0.03 x.

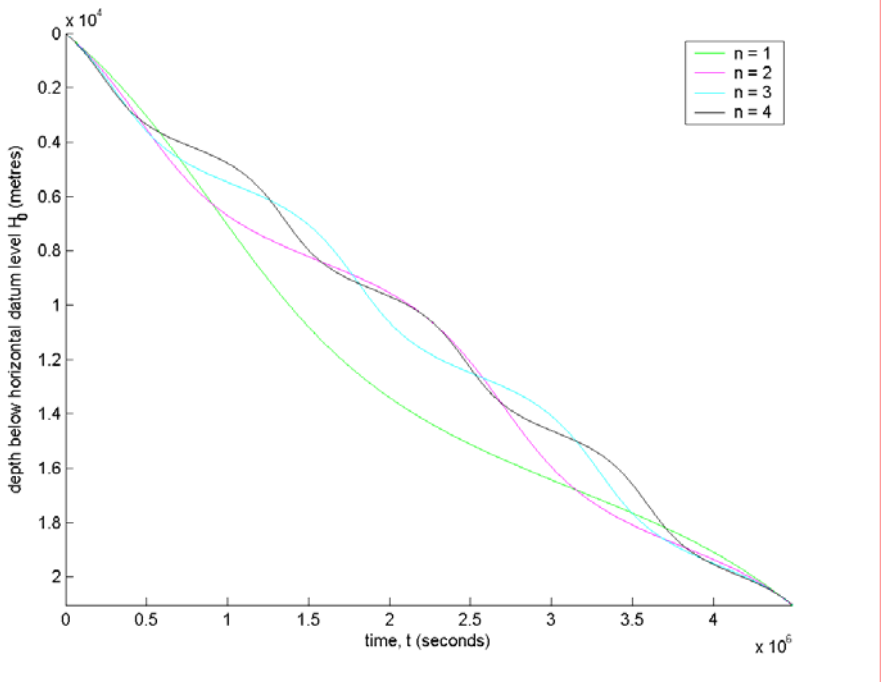

4.8. Results: Evolution of the flow

In this section, we use the numerical scheme given by (8) to calculate the evolution of the vertical thickness of the dense overflow along the characteristics and analyse the effects of topography. The flow is calculated along 59 characteristics in total, with characteristics 11 to 49 capturing the initial outflow. The extra characteristics allow for diffusive spreading of the flow. The drag coefficient, $r = 5 \times 10^{-6}$ s^{-1} and the model is run until $y = -10^6$, which is more realistic than the value used in Section 4.4.

Figures 4.12.(a)-(d) shows the flattening of the overflow water as it diffuses and spreads over the ocean floor in each case and this is highlighted in Figure 4.13. Over convex, concave and corrugated topography the cross sectional area of the outflow decreases significantly more than for constant slope topography. This may be due to the longer time taken for the outflow to traverse the topography as demonstrated in Figure 4.9. Figure 4.14 shows the cross sectional area decreasing as the number of corrugations and the distance the outflow covers increases.

In addition, the flow over concave and convex topography spreads further over the ocean bottom than for constant and corrugated topography. Flows with concave and convex bathymetry are also skewed upslope and downslope respectively. With concave bathymetry the characteristics furthest upslope take longer to reach a particular along slope distance than the characteristics further downslope, the opposite being true with convex bathymetry. This is a likely cause of the distortion in the shape of the flow with concave and convex bathymetry as parts of the outflow experience further dissipation during the additional time taken. With corrugated bathymetry the flow is also skewed upslope, again likely to be due to the longer time taken to traverse the bathymetry further downslope where the corrugations are larger (Figure 4.14).

Figure 4.12. The along slope evolution of the thickness of the dense overflow along the characteristics with (a) constant slope bathymetry. (b) concave slope bathymetry. (c) convex slope bathymetry. (d) corrugated slope bathymetry.

(a)

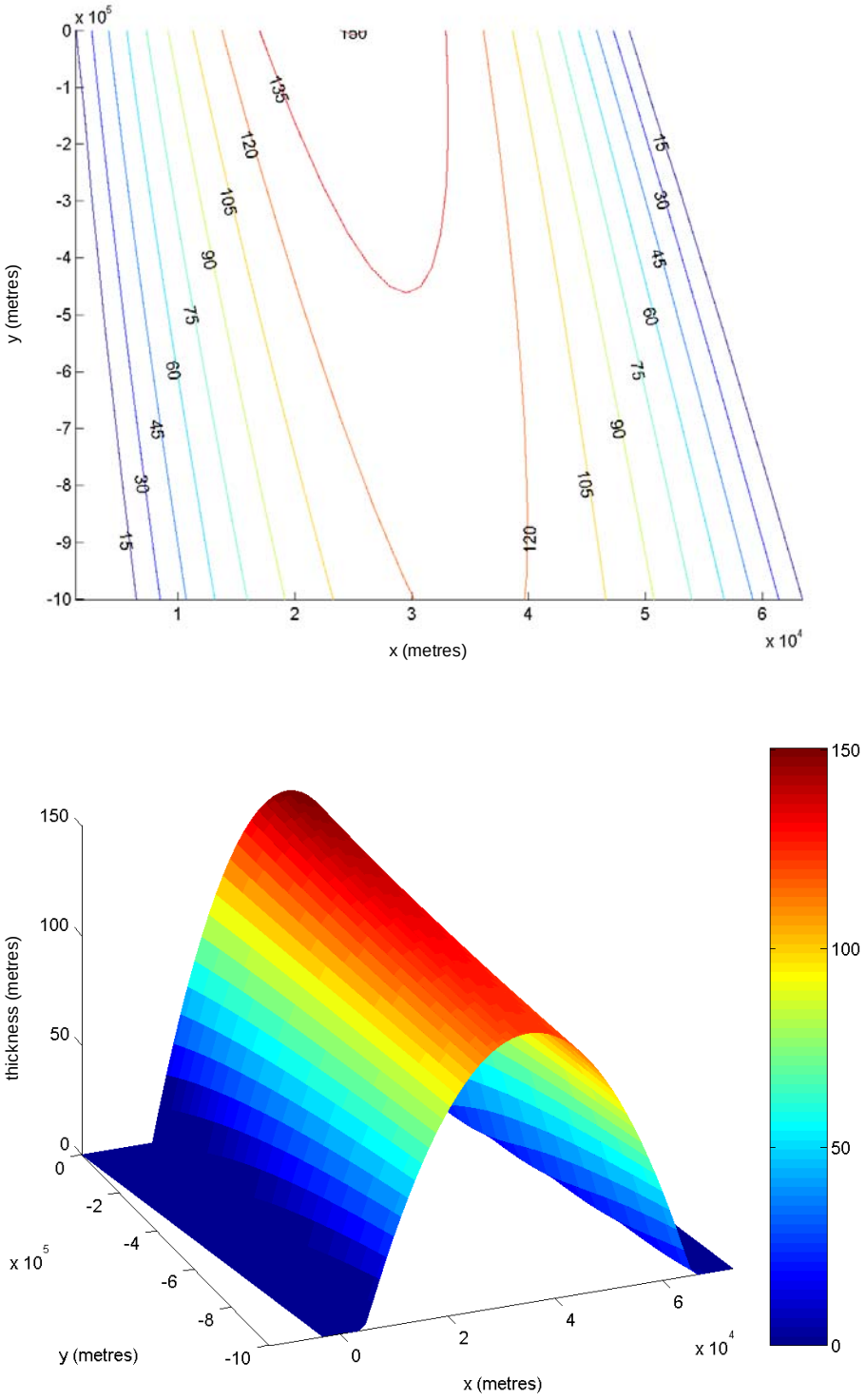

(b)

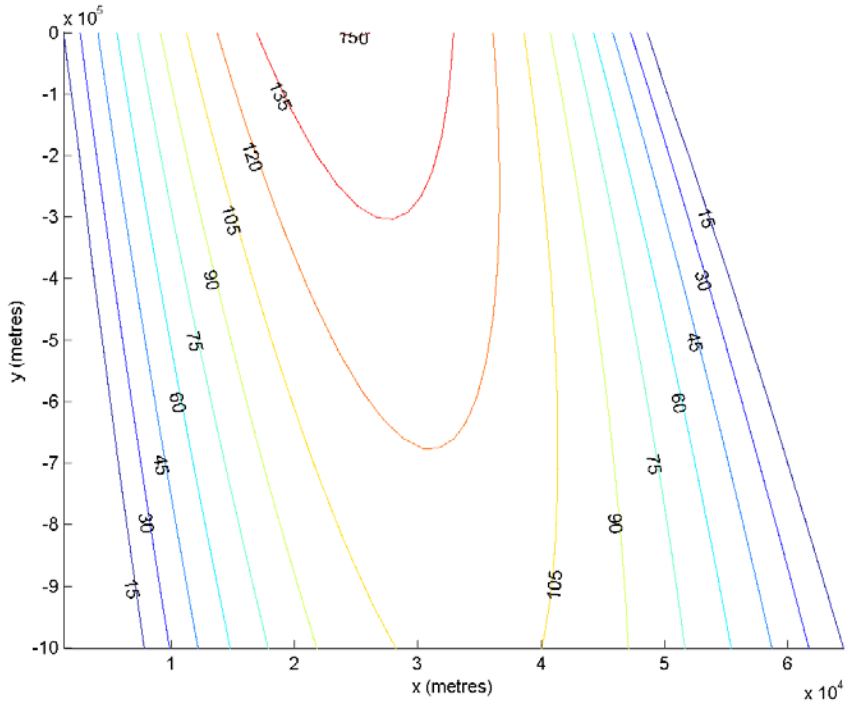
x 10^5
y (metres)
x (metres)
x 10^4
150
135
120
105
90
75
60
45
30
15

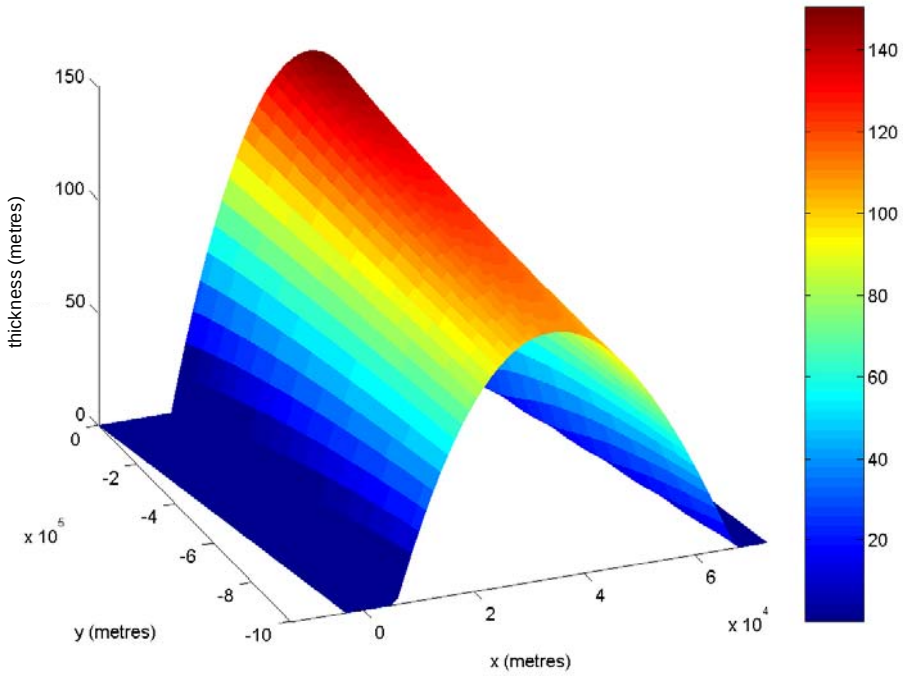
thickness (metres)
y (metres)
x 10^5
x (metres)
x 10^4
140
120
100
80
60
40
20

(c)

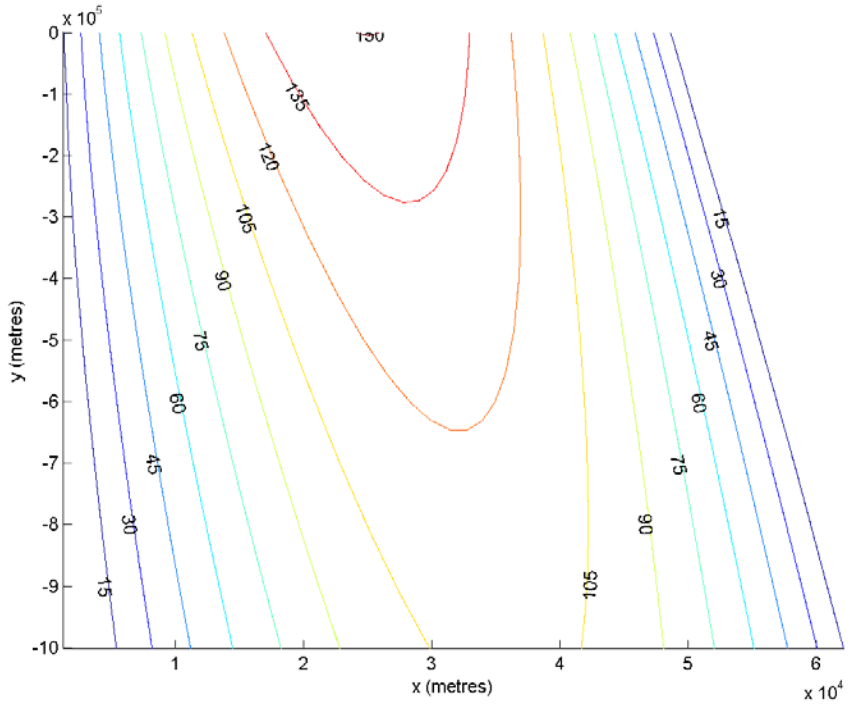
x 10^5
y (metres)
x (metres)
x 10^4
15
30
45
60
75
90
105
120
135
150

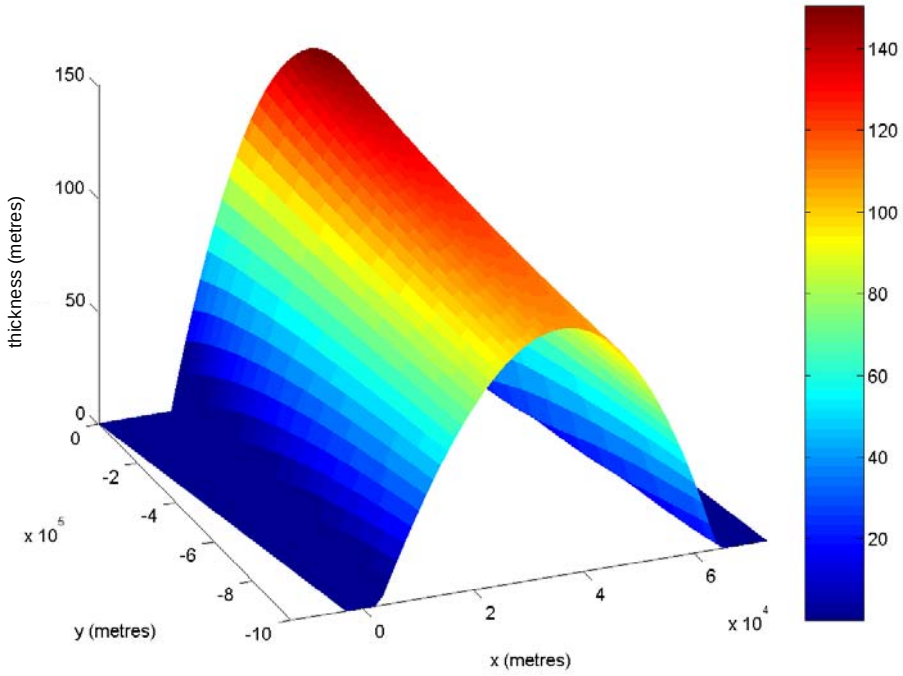
thickness (metres)
y (metres)
x 10^5
x (metres)
x 10^4

(d)

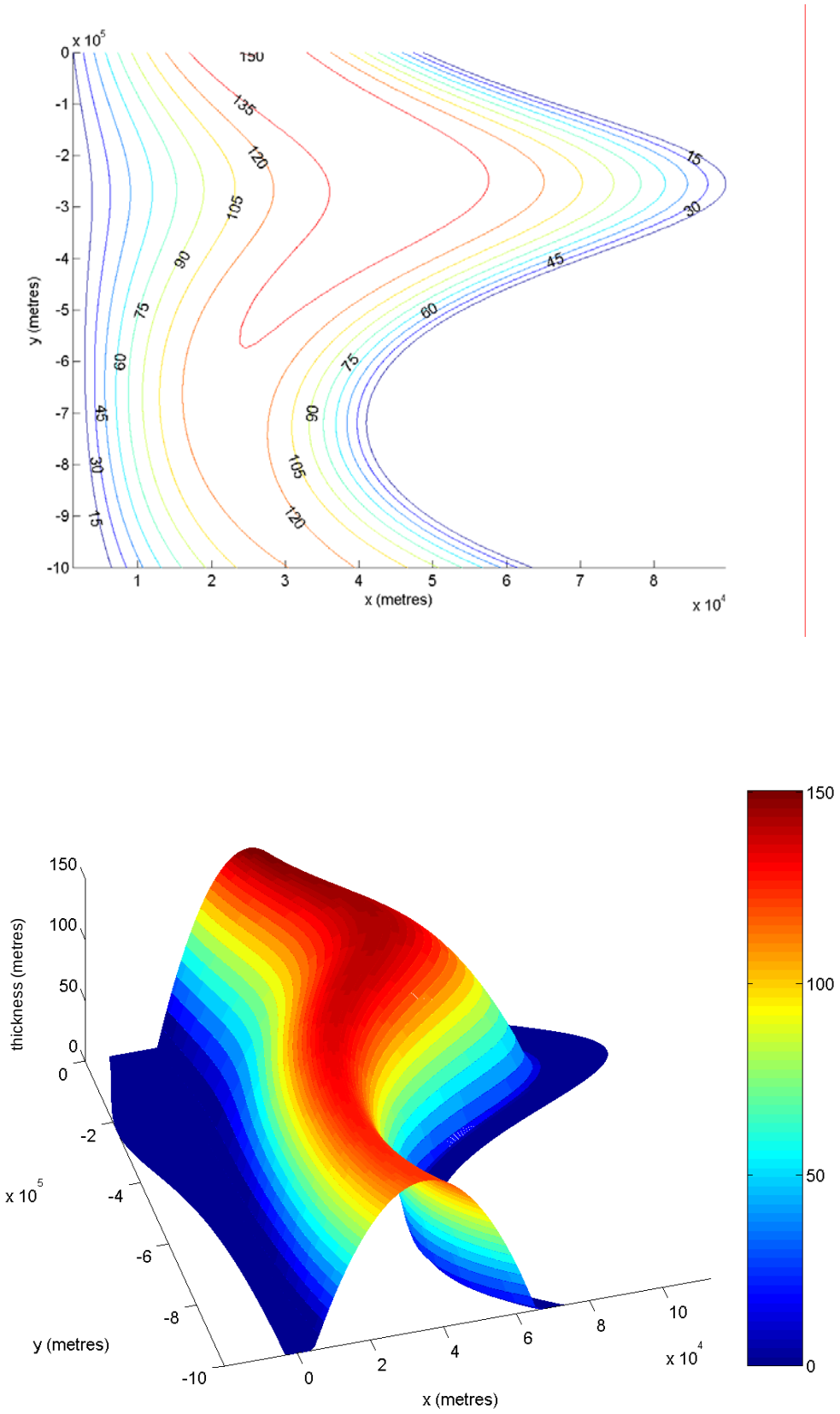
x 10^5
y (metres)
x (metres)
x 10^4
150
135
120
105
90
75
60
45
30
15
thickness (metres)
y (metres)
x (metres)
x 10^5
x 10^4

Figure 4.13. Comparison of the outflow thickness with different bathymetry at $y = -10^6$ (solid lines). The dotted line indicates the position of the outflow at $y = 0$ in all cases.

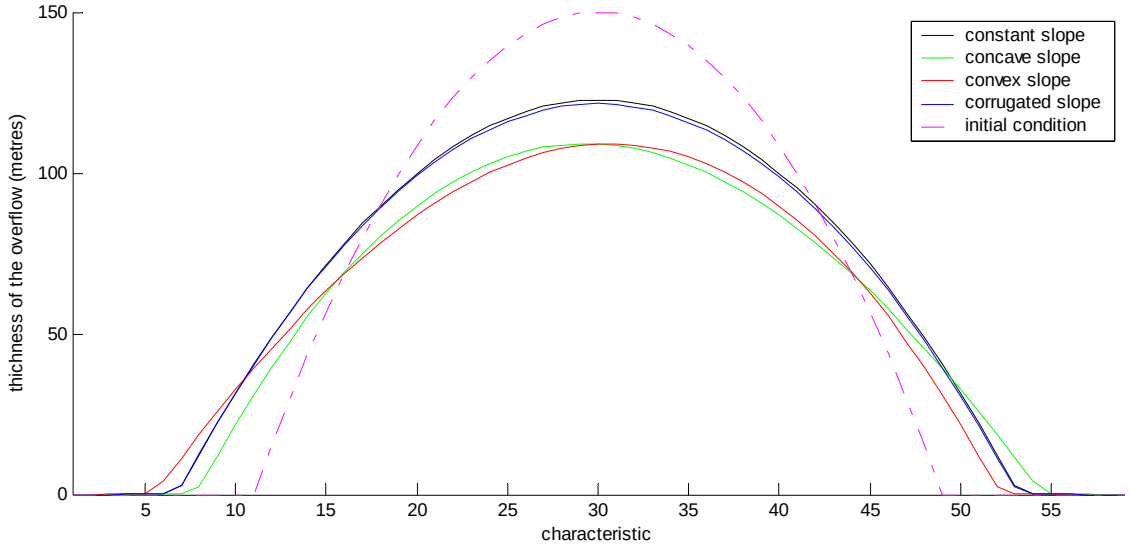

Figure 4.14. Comparison of the outflow thickness with varying n, the number of corrugations, at $y = -10^6$ (solid lines). Note that n = 0 is constant slope bathymetry.

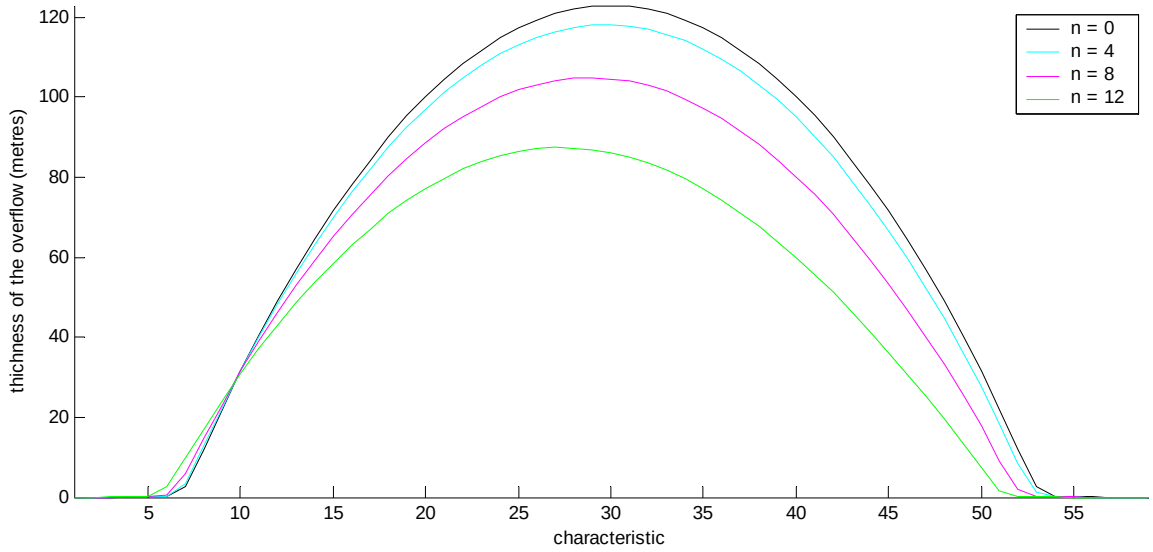

Chapter 5

Conclusions

We have provided an account of the main physical conditions and features that enable the formation of extremely dense surface waters. Slope convection is integral to abyssal water formation. Rigorous testing of theories on the dynamics of dense water overflows and cascades is currently not possible due to lack of available and complete observations. Theories supported by laboratory and numerical experiments suggest that the downslope transport of dense water on sloping bathymetry may occur as follows. A dense bottom flow descends under a balance of gravity, the Earth's rotation, bottom friction and turbulent entrainment. On sloping bathymetry, friction provides a more important component of the force balance due to increased gravitational acceleration. This allows an ageostrophic downslope component to the predominantly geostrophic alongslope flow. There are several further mechanisms resulting in downslope transport. Friction also allows downslope drainage of the dense flow in the bottom boundary layer. Eddies can be generated due to vortex stretching, which can disrupt the dense flow and break it up into a series of domes that propagate as coherent features on the slope. Experiments indicate that eddy transports are likely to facilitate the descent of dense fluid down the slope.

As the intensity of the source weakens, bottom friction provides an increasingly large contribution to the force balance, which alters the relative importance of these mechanisms. The downslope motion can be categorised into three regimes. An intense source is mostly geostrophically balanced, and may generate strong eddies. The contribution of Ekman drainage to downslope transport is relatively small. A moderate source still leads to predominantly geostrophic flow, but eddy production is suppressed and

Ekman drainage provides a larger component to the downslope flow. A weak source is viscously controlled and the only transport is drainage in the Ekman layer.

In addition, topography can alter the dynamical balance and features such as canyons may steer the dense flow rapidly downslope, or a topographic saddle point may possibly split the flow. Real topography on a scale comparable to topographic features that may affect the flow, such as canyons, is not currently known in these overflow regions. The thermobaric effect may also increase the velocity of very cold sinking water. Increased velocities result in corresponding increases in turbulent entrainment and detrainment, which act to dampen the enhanced dynamics and the final downslope penetration depends on the particular conditions.

Product water density is insensitive to variations in the source water density due to the strong damping by associated increases in entrainment. The details of the mixing process and the properties of the ambient water strongly control the properties of the product water, the depth of the downslope penetration and thus the depth of the overturning circulation. Entrainment varies along the path of the outflow, with stronger entrainment occurring over steeper regions. Entrainment of a number of overlying water masses leads to distinct product water characteristics. In a stratified environment, dense fluid is believed to be detrained from the plume. Quantifying entrainment, detrainment and the effects of stratification is an issue for future work. The potential role of sediments in cascading and transport amplification of dense surface waters has not been considered in much detail. Substantial amounts of sediments are available in European and Asian shelf regions. The enhancement of cascading by suspended sediments and mechanisms that account for their suspension is an area worth further research. Strong currents in the ambient seawater into which the overflow is flowing have an effect on the overflow. The influences of strong currents in the ambient ocean water were not considered, although they are known to affect overflows. The level of turbulence and friction can be controlled by tides or background alongslope currents and eddies can carry dense fluid out into the ambient circulation. Overflow transports should therefore not be considered in isolation from the background flow.

The contribution of episodic mesoscale cascades to abyssal water mass formation is another area for further study. Current estimates of cascade transport fluxes, when they are occurring, are comparable to those of wind-driven downwelling [Huthnance, 1995], and overflows and their associated transport processes, which are the main mechanisms that generate downslope motion at the ocean margin. Their significance is likely to be in the export of suspended and dissolved material or gasses such as phytoplankton, chlorophyll or carbon, rather than their contribution to the forcing of the thermohaline

circulation. The role of slope convention in maintaining essential exports of gasses, nutrients and pollutants etc. from productive shelf regions to the deep ocean is not considered in this study. It is likely to be highly important although current models of biogeochemical cycles cannot account for overflow fluxes and is another issue worth investigation.

A simple plume model was used to assess the role of bottom topography in determining the path, the rate of descent, and the evolution of the thickness and width of the outflow. The speed at which information is propagated along the characteristics depends entirely on the bottom topography. Variability in the gradient of the topography across the outflow distorts the characteristics and therefore the width of the outflow. Steeper regions do not allow the overflow to descend more quickly when an average gradient is maintained. The angle of descent is controlled by bottom drag, producing narrowing of the flow in troughs and widening over ridges. This occurs for features both in the along slope direction, such as for the troughs and ridges of corrugated bathymetry, and in the across slope direction, such as for the 'trough' of concave bathymetry. Variable topography across the outflow also affects the shape of the flow. Parts of the flow can travel different distances and at various speeds. This affects the amount of dissipation of the dense water across the outflow, subsequently altering the flow thickness a variable amount across the flow.

Although this simple model is useful for analytic purposes and can illustrate the effects of bottom topography, it is not realistic in several respects. Once initialised, the model outflow is determined only by the model dynamics and the bottom topography. The dynamics of the outflow are assumed to be completely separate from those of the surrounding ocean, which may be appropriate when the currents in the outflow are much larger than the currents in the overlying ocean. However, the evolution of the model outflow is also independent of its own properties as well as those of its oceanic environment, and is severely limited in this respect. The temperature and salinity of the flow, both affecting density, are not included and the only driving force is reduced gravity. Entrainment and other mixing processes indispensable to density current dynamics are ignored and the broadening of the outflow is solely due to the diffusion term. The linear frictional drag parameterises complex turbulent processes occurring within overflows and their interaction with the seafloor. The model clearly cannot give insight into many other aspects of the dynamics of dense water overflows, such as changes in properties along the path of the outflow or the horizontal structure of a real outflow. Although this model is highly simplified, its representation of a dense water overflow may have some value in describing of behaviour of overflows in dissipative climate models. Given the vastly important role of dense overflow dynamics, this highlights the need for improvement of their representation in current models.

Due to time constraints, there remain many improvements to be made to the model and a large amount still to be investigated. The numerical scheme could be improved using a full conservative form and, for example, a Runge-Kutta scheme. Comprehensive convergence testing also needs to be completed. More realistic bottom drag can easily be incorporated using a quadratic friction term. Entrainment of overlying lighter water could also be added and the effects investigated. Although beyond the scope of the present study, real bottom topography, and oceanic temperature and salinity profiles, could be incorporated.

Notation

h	Vertical thickness of the dense layer	m
H	Depth of the topography from the sea surface	m
H_0	Horizontal datum level	m
ρ_0	Density of the unstratified ambient fluid	kg m^{-3}
$\Delta\rho$	Density excess	kg m^{-3}
r	Drag coefficient	s^{-1}
p	Pressure	m^{-1} kg s^{-2}
g'	Reduced acceleration due to gravity	m s^{-2}
f	Coriolis parameter	s^{-1}
$\underline{u}$	Horizontal velocity	m s^{-1}
$\underline{u}_c$	Characteristic velocity	m s^{-1}
$\underline{k}$	Unit vector in the z direction	
a	Amplitude of the corrugation	m
k	Period of the corrugation	m
n	Number of periods of corrugation	

Acknowledgements

I would like to thank Professor David Marshall for his help, contribution and time. Thanks also to Owen, my course mates, and the financial support received from NERC that enabled me to complete this course.

References

Backhaus, J.O., Fohrmann, H., Kämpf, J. and Rubino, A. (1997) 'Formation and export of water masses produced in Arctic shelf polynyas – process studies of oceanic Convection', *ICES Journal of Marine Science*, 54, 366–382.

Baines, P.G. and Condie, S. (1998) 'Observations and Modelling of Antarctic Downslope Flows: A Review' in *Ocean, ice and atmosphere: Interactions at the Antarctic Continental Margin*, Antarctic Research Series, 75, 29-49.

Baringer, M.O. n.d., *Overflows in the Atlantic*, [online] Available: http://www.aoml.noaa.gov/general/project/phodmob2.html (2004, July 24).

Bauch, D., Schlosser, P., Fairbanks, R.G. (1995) 'Fresh-water balance and the sources of deep and bottom waters in the Arctic Ocean inferred from the distribution of (H20)-O-18', *Progress in Oceanography*, 35 (1), 53-80.

Bruce, J.G. (1995) 'Eddies southwest of the Denmark Strait', *Deep-Sea Research*, 42, 13-29.

Cenedese, C., Whitehead, J.A., Ascarelli, T.A. and Ohiwa, M. (2004) 'A dense current flowing down a sloping bottom in a rotating fluid', *Journal of Physical Oceanography*, 34(1), 188-203.

Chapman, D.C. and Gawarkiewicz, G. (1995) 'Offshore transport of dense shelf water in the presence of a submarine canyon', *Journal of Geophysical Research*, 100, 13373-13387.

Clarke, R. A. and Gascard, J.C. (1983) 'The formation of Labrador Sea Water. Part I: Large-scale Processes', *Journal of Physical Oceanography*, 13, 1764-1778.

Condie, S.A. (1995) 'Descent of dense water masses along continental slopes', *Journal of Marine Research*, 53, 897-928.

Dickson, R.R. and Brown, J. (1994) 'The production of North Atlantic Deep Water: sources, rates and pathways', *Journal of Geophysical Research*, 99, 12319-12341.

Döscher, R. and Redler, R. (1997) 'The relative importance of northern overflow and subpolar deep convection for the North Atlantic thermohaline circulation', *Journal of Physical Oceanography*, 27 (9), 1894-1902.

Encyclopædia Britannica Premium Service, n.d., Continental Slope, [online] Available: http://www.britannica.com/eb/article?eu=2648 (2004, August 9).

Etling, D., Gelhardt, F., Schrader, U., Brennecke, F., Kuhn, G., d'Hieres, G.C. and Didelle, H. (2000) 'Experiments with density currents on a sloping bottom in a rotating fluid', *Dynamics of Atmospheres and Oceans*, 31 (1-4), 139-164.

Ezer, T. (2004) 'Entrainment, diapycnal mixing and transport in three-dimensional bottom gravity current simulations using the Mellor–Yamada turbulence scheme', (in print).

Fogelqvist E, Blindheim J, Tanhua T, Osterhus S, Buch E, Rey F (2003) 'Greenland-Scotland overflow studied by hydro-chemical multivariate analysis', *Deep-Sea Research Part I*, 50 (1), 73-102.

Gill, A. E., (1973) 'Circulation and bottom water production in the Weddell Sea', *Deep-Sea Research,* 20, 111–140.

Gill, A.E. (1982) *Atmosphere Ocean Dynamics*, Academic Press, New York.

Gawarkiewicz, G. and Chapman, D.C. (1995) 'A numerical study of dense water formation and transport on a shallow, sloping continental shelf', *Journal of Geophysical Research-Oceans*, 100 (C3), 4489-4507.

Girton, J.B. and Sanford, T.B., (2003) 'Descent and modification of the overflow plume in the Denmark Strait', *Journal of Physical Oceanography*, 33, 1351–1364.

Griffies, S.M., Boning, C., Bryan, F.O., Chassignet, E.P., Gerdes, R., Hasumi, H., Hirst, A., Treguier, A. and Webb, D. (2000) 'Developments in ocean climate modelling', *Ocean Modelling*, 2, 123–192.

Hill, A.E., Souza, A.J., Jones, K., Simpson, J.H., Shapiro, G.I., McCandliss, R., Wilson, H. and Leftley, J. (1998) 'The Malin cascade in winter 1996', *Journal of Marine Research*, 56 (1), 87-106.

Huthnance, J.M. (1995) 'Circulation, exchange and water masses at the ocean margin: the role of physical processes at the shelf edge', *Progress in Oceanography*, 35, 353-431.

Ivanov, V.V., Shapiro, G.I., Huthnance, J.M., Aleynik, D.L., Golovin, P.N. (2004) 'Cascades of dense water around the world ocean', *Progress in Oceanography*, 60 (1), 47-98.

Jiang, L. and Garwood, R.W. (1996) 'Three-dimensional simulations of overflows on continental shelves', *Journal of Physical Oceanography*, 26, 1214-1233.

Jiang, L. and Garwood, R.W. (1995) 'A numerical study of three-dimensional dense bottom plumes on a Southern Ocean continental slope', *Journal of Geophysical Research*, 100, 18471-19488.

Jiang, L. and Garwood, W., (1998) 'Effects of topographic steering and ambient stratification on overflows on continental slopes: A model study', *Journal of Geophysical Research***,** 103 (C3), 5459–5476.

Jones, H. n.d., *Open-Ocean Deep Convection*, [online] Available: http://puddle.mit.edu/~helen/oodc.html (2004, August 10)

Jungclaus, J.H. and Backhaus, J.O., (1994) 'Application of a transient reduced gravity plume model to the Denmark Strait overflow', *Journal of Geophysical Research*, 99 (C6), 12375–12396.

Jungclaus, J.H., Backhaus, J.O., Fohrmann, H. (1995) 'Outflow of dense water from the Storfjord in Svalbard: a numerical model study', *Journal of Geophysical Research*, 100 (C12), 24719-24728.

Kampf, J. and Fohrmann, H. (2000) 'Sediment-driven downslope flow in submarine canyons and channels: Three-dimensional numerical experiments', *Journal of Physical Oceanography*, 30 (9), 2302-2319.

Killworth, P.D. (1977) 'Mixing on the Weddell Sea continental slope', *Deep-Sea Research*, 24, 427-448.

Killworth, P.D. (1983) 'Deep convection in the world ocean', *Reviews of Geophysics and Space Physics*, 21 (1), 1-26.

Killworth, P.D. (2001) 'On the rate of descent of overflows', *Journal of Geophysical Research*, 106 (C10), 22267-22275.

Krauss, W. (1996) 'A note on overflow eddies', *Deep-Sea Research*, 43, 1661-1667.
Lane-Serff, G.F. and Baines, P.G. (1998) 'Eddy formation by dense flows on slopes in a rotating fluid', *Journal of fluid mechanics*, 363, 229-252.

Lane-Serff, G. (2001) 'Overflows and cascades' in Steele, J.H. (ed.), *Encyclopaedia of ocean sciences*, Academic Press, New York.

Latif, M. A., Ozsoy, E., Oguz, T. and Unluata, U. (1991) 'Observations of the Mediterranean outflow into the Black Sea', *Deep-Sea Research,* 38 (2), 711-723.

Lazier, J., Pickart, R. and Rhines, P. (2001) 'Deep convection' in Seidler, G., Church, J. and Gould, J. (eds.) *Ocean Circulation and Climate*, London, Academic Press.

Legg, S., Hallberg, R.W. and Girton, J.B. (2004) 'Comparison of entrainment in overflows simulated by z-coordinate, isopycnal and nonhydrostatic models', (in press).

Løyning, T.B. and Weber, J.E. (1997) 'Thermobaric effect on buoyancy-driven convection in cold seawater', *Journal of Geophysical Research*, 102 (C13), 27875-27885.

Lundberg, P. A. (1983) 'On the mechanics of deep water flow in the Bornholm Channel', *Tellus,* 35**,** 149–158.

Muench, R.D. and Gordon, A.L. (1995) 'Circulation and transport of water along the western Weddell Sea margin', *Journal of Geophysical Research*, 100, 18503-18515.

Nof, D. (1983) 'The translation of isolated cold eddies on a sloping bottom' *Deep-Sea Research Part A*, 30 (2), 171-182.

Özgökmen, T.M. and Chassignet, E.P. (2002) 'Dynamics of Two-Dimensional Turbulent Bottom Gravity Currents', *Journal of Physical Oceanography*, 32 (5), 1460–1488.

Price, J.F. (1992) 'Overflows: the source of new abyssal ocean waters', *Oceanus*, 35, 11-34.

Price, J.F., Baringer, M.O., Lueck, R.G., Johnson, G.C., Ambar, I, Parrilla, G., Cantos, A., Kennelly, M.A., Sanford, T.B. (1993) 'Mediterranean outflow mixing and dynamics', *Science*, 259 (5099), 1277-1282.

Price, J.F. and O'Neil Baringer, M. (1994) 'Outflows and deep water production by marginal seas', *Progress in Oceanography*, 33, 161-200.

Quadfasel, D., Rudels, B. and Kurz, K. (1988) 'Outflow of dense water from a Svalbard fjord into the Fram Strait', *Deep-Sea Research*, 35, 1143–1150.

Quadfasel, D., Rudels, B. and Selchow, S. (1992) 'The central bank vortex in the Barents Sea: water mass transformation and circulation', *ICES Marine Science Symposium*, 195, 40–51.

Rudels, B., and Quadfasel, D. (1991) 'Convection and deep water formation in the Arctic Ocean-Greenland Sea system', *Journal of Marine Systems*, 2, 435–450.

Rudels, B., Jones, E.P. and Anderson, L.G. (1994) 'On the Intermediate Depth Waters of the Arctic Ocean' in Johannessen, O.M., Muench, R.D., Overland, J.E. (eds.), *The Polar Ocean and their Role in Shaping the Global Environment Vol. 85*, American Geophysics Union, Washington, DC, 33-46.

Rudels, B., Friedrich, H.J. and Quadfasel, D. (1999) 'The Arctic circumpolar boundary current', *Deep-Sea Research Part II* , 46, 1023–1062.

Saunders, P.M. (2001) 'The Dense Northern Overflows' in Seidler, G., Church, J. and Gould, J. (Eds.) *Ocean Circulation and Climate*, London, Academic Press, 401-417.

Seung,Y.H. (1987) 'A buoyancy flux-driven cyclonic gyre in the Labrador Sea', *Journal of Physical Oceanography*, 17, 134-146.

Shapiro, G.I. and Hill, A.E. (1997) 'Dynamics of dense water cascade at the shelf edge', *Journal of Physical Oceanography*, 33, 390–406.

Shapiro, G.I. and Zatsepin, A.G. (1997) 'Gravity current down a steeply inclined slope in a rotating fluid', *Annual Review of Geophysics*, 15, 366-374.

Shapiro, G.I., Huthnance, J.M. and Ivanov, V.V. (2003) 'Dense water cascading off the continental shelf', *Journal of Geophysical Research*, 108 (C12), 3390.

Schauer, U. (1995) 'The release of brine enriched shelf water from Storfjord to the Norwegian Sea', *Journal of Geophysical Research*, 100, 16015-16028.

Schauer, U. and Fahrbach, E. (1999) 'A dense bottom water plume in the western Barents Sea: downstream modification and interannual variability', *Deep-Sea Research Part I*, 46, 2095-2108.

Smith, P.C. (1975) 'A streamtube model for bottom boundary currents in the ocean', *Deep-Sea Research*, 22, 853-873.

Smith, P.C. (1977) 'Experiments with viscous source flows in rotating systems', *Dynamics of the Atmospheres and Oceans*, 1, 241-272.

Tanaka, K. and Akitomo, K. (2001) 'Baroclinic instability of density current along a sloping bottom and the associated transport process', *Journal of Geophysical Research*, 106 (C2), 2621-2638.

Tomczak, M. (1985) 'The Bass Strait water cascade during winter 1981', *Continental Shelf Research*, 4, 255–278.

Toole, J.M., Polzin, K.L. and Schmitt, R.W. (1994) 'Estimates of diapycnal mixing in the abyssal ocean', *Science,*264, 1120-1123.

Whitehead, J.A. (1993) 'A laboratory model of cooling over the continental shelf', *Journal of Physical Oceanography***,** 23, 2412–2427.

Willebrand, J., Barnier, B., Böning, C., Dieterich, C., Killworth, P.D., Provost, C., Jia, Y., Molines, J. and New, A.L. (2001) 'Circulation characteristics in three eddy-permitting models of the North Atlantic', *Progress in Oceanography*, 48 (2-3), 123-161.

Wunsch, C. and Ferrari, R. (2004) ‘Vertical mixing, energy and the general circulation of the oceans’, *Annual Review of Fluid Mechanics*, 36, 281-314.

Zoccolotti, L., and Salusti, E. (1987) ‘Observations of a vein of very dense marine water in the southern Adriatic Sea’ *Continental Shelf Research*, 7**,** 535–551.